

Article

# Sedimentary Facies Analysis, Reservoir Characteristics and Paleogeography Significance of the Early Jurassic to Eocene Carbonates in Epirus (Ionian Zone, Western Greece)

George Kontakiotis \*, Leonidas Moforis \*, Vasileios Karakitsios and Assimina Antonarakou

Department of Historical Geology and Paleontology, Faculty of Geology and Geoenvironment, National and Kapodistrian University of Athens, Panepistimiopolis, 15784 Athens, Greece; vkarak@geol.uoa.gr (V.K.); aantonar@geol.uoa.gr (A.A.)

\* Correspondence: gkontak@geol.uoa.gr (G.K.); leomof@geol.uoa.gr (L.M.); Tel.: +30-2107274804 (G.K.)

Received: 27 August 2020; Accepted: 10 September 2020; Published: 11 September 2020

**Abstract:** Sedimentological, micropalaeontological, and marine geological results from the Early Jurassic to Eocene carbonate formations of the Ionian zone, from six localities of Epirus, provide new insights into the basin palaeogeographic evolution and better correlation with coeval analogous tectono-stratigraphic successions along the southern margin of the Neo-Tethys Ocean. Facies analysis allowed the recognition of several microfacies types and their depositional characteristics. During the Early Jurassic, autochthonous carbonates (Pantokrator Limestones) were deposited in shallow-water environment. The overlying (hemi)pelagic Siniais or their lateral equivalent Louros Limestones were deposited to the basin borders and mark the general deepening of the Ionian domain. During Toarcian to Tithonian, the Ionian Basin was characterized by an internal differentiation in small sub-basins with half-graben geometry presenting abrupt thickness and facies changes. The deeper parts were characterized by continuous sedimentation, while the elevated parts were marked by unconformities. The Early Cretaceous marks the homogenization of sedimentation by the deposition of the pelagic Vigla Limestones all over the Ionian zone. The transition from the Early to Late Cretaceous records a significant carbonate diversification in terms of biota assemblages, and related mineralogy due to intense tectonic activity in the region. From Late Cretaceous to Paleogene, allochthonous carbonates were transported to the outer shelf by turbidity currents (calciturbidites) and/or debris flows (limestones with breccia) formed by the gravitational collapse of the platform margin. Additional porosity and bulk density measurements showed that petrophysical behavior of these carbonates are controlled by the depositional environment and further influenced by diagenetic processes. The partly dolomitized neritic Jurassic carbonates, but mainly the Senonian calciturbidites and the microbrecciated Paleocene/Eocene limestones display the higher average porosity values, and therefore present enhanced carbonate reservoir quality.

**Keywords:** microfacies types; Pantokrator Limestones; Vigla Formation; Senonian calciturbidites; Eocene brecciated limestones; carbonate porosity; petroleum prospectivity; stratigraphic correlations; marine biogenic carbonates; depositional environment

---

## 1. Introduction

Marine biogenic carbonates are among the most important archives of Earth's history reflecting past changes in ocean chemistry, water mass circulation and the evolution of life [1–10]. Particularly

during the Cretaceous, changes in climate, oceanographic circulation, sea level, tectonic and volcanic activity contributed to triggering widespread crisis events, which resulted in world-wide anoxic episodes [11–17], drastic facies variations and biotic changes [18–23], and diffusion of bauxite deposits [24,25], among others. Such complex events were reflected on biotic and non-biotic constituents of the carbonate platforms and on the architecture of their depositional systems.

Within the Mediterranean Tethys (Neo-Tethys) Ocean, the Mesozoic-Paleogene Eras witnessed the development of vast carbonate platform belts that fringed its margins and passed into deep marine equivalents, completing thus the marginal succession in the deeper parts of the basin [26–29]. These successions, including the slope deposits in the platform margins, provide an excellent example of the evolution of depositional sequences ranging from the platform through rimmed carbonate-shelf to pelagic depositional settings, and further characterize long intervals in the rifting and subsidence history of past peri-Tethyan continents. Among them, the carbonate platform to basin transition can give rise to fragmentary distribution of marginal slope successions as fault-bounded units [30–32]. Such confined carbonate units are also considered to be aquifer systems, hydraulically independent of their siliciclastic cover, and therefore, can build prolific reservoirs and become potential exploration targets for oil and gas throughout the entire Mediterranean basin.

Within the Ionian Zone, both the Early Jurassic neritic limestones and dolomites, and the Late Cretaceous to Eocene re-sedimented carbonates (calcareous turbidites and coarser breccia) are considered the main reservoir successions and exploration targets for oil and gas in western Greece [33–35], central and southern Adriatic offshore Italy [36,37], and onshore Albania [35,38–40]. The Jurassic karstified platform carbonate facies represent an excellent analogue for the carbonate reservoirs, where the sea-level drawdown and subaerial exposure of the carbonate reef enhanced the facies reservoir quality. Moreover, the calciturbidites can be of great economic importance and they can serve as reservoir rocks [39,41,42], due to their high porosity and bulk density values, which can be additionally enhanced by the development of chert nodules [43]. However, the nature and distribution of these deposits along with their depositional mechanism processes and environmental conditions, especially in western Greece, are still poorly constrained. The high heterogeneity related to fabric, texture, fractures that usually characterize such kind of reservoirs has been highlighted by several authors [42,44–51]. Understanding heterogeneity of carbonate reservoir helps predicting reservoir petrophysical and geomechanical behaviors [52–54], which in turn play a crucial role in their exploration, production, and development [55–57]. In this regard, high-resolution sedimentological outcrop data are essential, because they help to fill the gap with respect to subsurface data, which assists in refining reservoir models. Petrographic constraints based on facies analysis provide sedimentological features and micro-textural characteristics, which are the key-link between the rock depositional/diagenetic history and its physical properties.

In the present study, we introduce a complete record of the marginal successions in the western (Ionian basin) segment of the southern Tethys, which consists of the Early Jurassic to Eocene carbonate platform and slope to basin successions from the Epirus region (Figure 1). This integrated study aims to define the Mesozoic-Paleogene depositional history, based on lithostratigraphic characteristics and reservoir petrophysical behaviors in the central Ionian domain, a major hydrocarbon prolific basin in western Greece. This was accomplished by detailed sedimentological and geomechanical/petrophysical analyses of the carbonate succession, in conjunction with a synthetic paleogeographic reconstruction. Beyond the hydrocarbon prospectivity, this work has further implications for regional geology, since it contributes to describing the evolution of these carbonates, and to a better understanding of the Ionian zone (pre-, syn- and post-rift stages; [34,58]) in western Greece, a region with crucial economic and strategic importance.

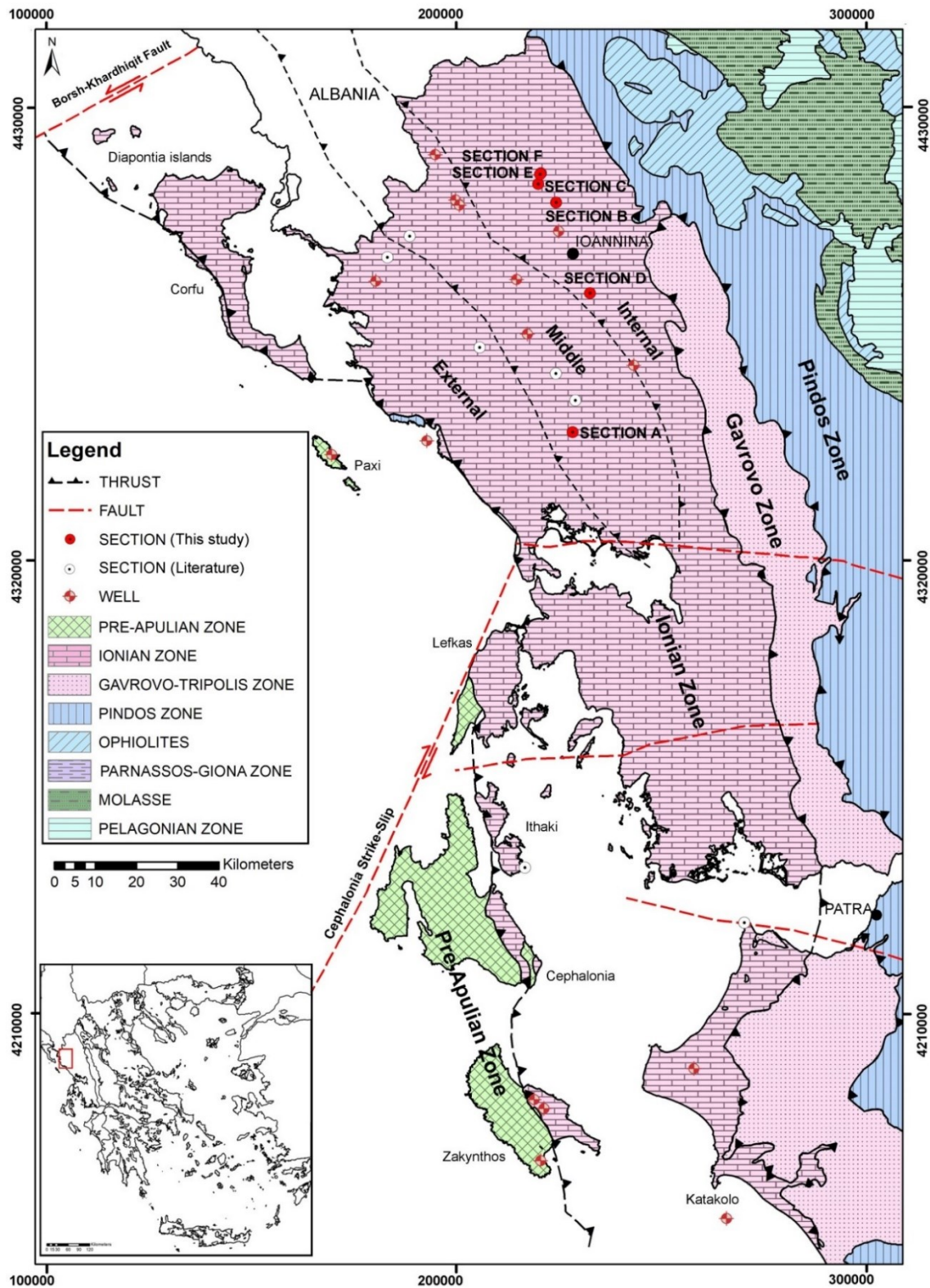


**Figure 1.** Geological map of the external Hellenides in NW Greece (modified from [34,35]) illustrating the principal tectonostratigraphic zones: Pre-Apulian, Ionian, Gavrovo, Pindos. The red box shows the study area, the northwestern part of the Epirus region, where the separation of Ionian zone to external, middle, and internal sub-basins along with the regional locations of the study sections to be also indicated. Legend interpretations are presented in the inset.

## 2. Geological Setting

### 2.1. Tectonostratigraphic Evolution of Ionian Basin

Western Greece is dominated by the external zones of the Hellenides fold-and-thrust belt, namely the pre-Apulian, Ionian and Gavrovo-Tripolis zones. At a regional scale (hundreds of kilometers), this Alpine belt records the initiation, development and final destruction of the southeastern margin of the Tethys Ocean and the consequent continent-continent collision between the Apulian and Pelagonia micro-continents to the east [34,58–63]. On a smaller scale (tens of kilometers), the various sub-basins of the Hellenic Tethyan margin have been inverted to produce the main Hellenic thrust sheets or folded zones [58,59,64]. The Ionian zone, which is bounded westwards by the Ionian thrust and eastwards by the Gavrovo thrust, extends from Albania to the north, forms most of the Epirus region and parts of the Ionian islands and continues southwards to central Greece, Crete and the Dodecanese. According to [65,66], the Ionian basin was subdivided into the internal, central and external Ionian sub-basins (Figure 1).

The tectonostratigraphic evolution of the Ionian zone is reflected on the deposition of three distinct sequences indicative of different tectonic regimes [34,58]: (1) a pre-rift sequence is represented by the Early Jurassic platform Pantokrator Limestones, which overly Early to Mid-Triassic evaporites through Foustapidima Limestones of Ladinian-Rhetian age, (2) a syn-rift sequence (Pliensbachian-Tithonian) deposited during extensional faulting and halokinesis of the Triassic evaporites, which caused the formation of the Ionian basin and its internal synrift differentiation into smaller sub-basins characterized by asymmetric half-graben geometry and different carbonate thickness accumulation [42,58]. Complete Toarcian-Tithonian syn-rift pelagic sequences (Siniais and lateral equivalent Louros Limestones, Ammonitico Rosso or lower Posidonia beds, Limestone with filaments, Upper Posidonia beds) are located in the deeper part of the half-grabens, while unconformities interrupt these sequences in the rift shoulders, (3) a post-rift sequence (Early Cretaceous-Eocene) deposited after the cessation of extensional faulting, is defined by a synchronous throughout the basin Early Berriassian break-up, which is marked by an unconformity at the base of the pelagic Vigla Limestones. The Mesozoic to Eocene carbonate succession passes upwards to the flysch synorogenic sedimentation (siliciclastic turbidites), which began at the Eocene–Oligocene boundary and revealed progressively diminishing thicknesses from the internal to the external areas. Until the Early Miocene, the basin was filled with submarine fan deposits, in response to movement of Pindos thrust, compressional structures, deformation of the external Hellenides which migrated westwards, uplift of the entire Hellenides orogenic belt, and development of a foreland basin at the edge of the Apulian microcontinent [67–71].

### 2.2. Lithostratigraphy of Jurassic-Eocene Formations in the Ionian Basin

All the study sections are situated within the middle-internal Ionian Zone, in Epirus region near Ioannina (Figure 2A–E). They represent to the Mesozoic-Paleogene pre- to post-rift sequences of Ionian zone, and particularly the upper part of Early Jurassic Pantokrator Limestones, the pelagic Early Cretaceous Vigla Limestones, the Late Cretaceous Senonian Limestones, and the microbreccious limestones of Paleocene/Eocene age. These formations are described in stratigraphic order as follows:

#### 2.2.1. Pantokrator Limestones and Lateral Equivalents

Early Jurassic (Hettangian to Sinemurian) Pantokrator Limestones represent the upper part of the pre-rift sequence of the Ionian zone [64,72]. This formation can be described as a neritic formation, consisted of limestones and dolomites with calcareous algae and benthic foraminifera of more than 1000 m of total thickness. These shallow-water limestones overlie Early to Middle Triassic evaporites (>2000 m thick) and the Foustapidima Limestones of the Ladinian–Rhaetian. Due to their remarkable facies' homogeneity, such Jurassic marine deposits represent an extensive carbonate platform at that time covering the entire region from the Apulian to the Gavrovo zone [58]. The overlying syn-rift

sequence in the deeper part of the half-graben sub-basins begins with the Pliensbachian pelagic Siniais Limestones and its lateral equivalent Louros Limestones (both indicative of the first deepening event of the Ionian basin), overlain in some sub-basins by the succession “Ammonitico Rosso”, “Limestones with filaments”, and “Upper Posidonia Beds”, while in others, the “Ammonitico Rosso” is replaced by the coeval “Lower Posidonia Beds” in the previous sequence, or even the whole sequence is represented by the undifferentiated Posidonia Beds [34,58]. The boundary between the Pantokrator Limestones and Louros or Siniais Limestones is gradational.

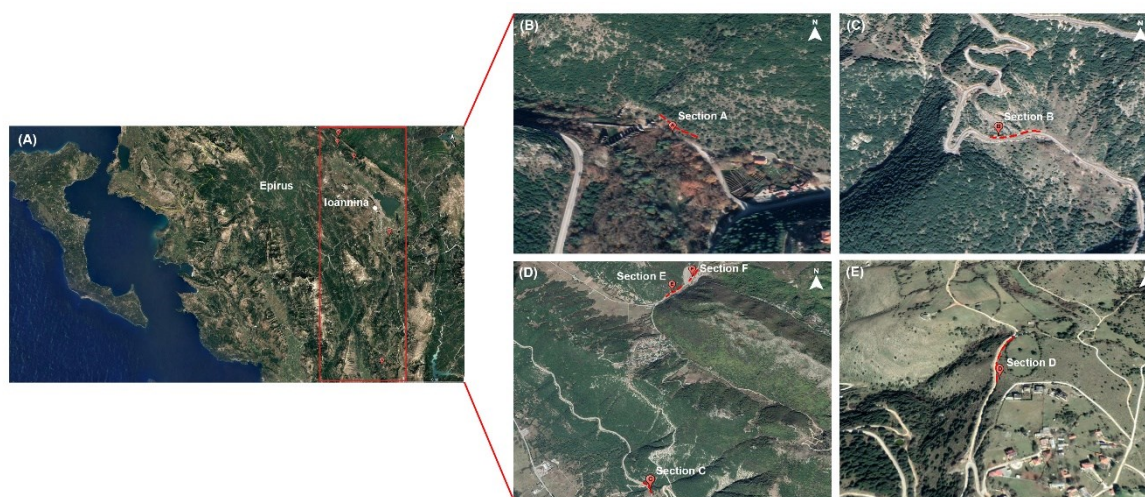


**Figure 2.** Google Earth maps of (A) Studied region in Epirus (NW Greece) into the red box; (B) Agios Georgios section (lat: 39°16'14.99" N, lon: 20°50'59.43" E); (C) Perivleptos section (lat: 39°46'21.90", lon: 20°46'48.34" E); (D) Vigla (lat: 39°48'33.45" N, lon: 20°43'38.73" E), Asprageli-1 (lat: 39°45'57.42" N, lon: 20°43'58.25" E) and Asprageli-2 (lat: 39°49'54.00" N, lon: 20°43'58.25" E) sections; (E) Koloniati section (lat: 39°34'52.46" N, lon: 20°53'11.41" E). The orange symbols mark the locations of the six study sections, and red dashed lines correspond to the major studied outcrops respectively.

### 2.2.2. Vigla Formation

This pelagic formation can be described as sub-lithographic thin-bedded to platy deposits, rich in planktonic organisms (*Calpionelles*, *Radiolaires*, and *Globotruncanes*) of Cretaceous age. Their continuity is usually interrupted by thin intercalations, chert lenses, or even thin chert layers. Its dominant lithology consists of light grey to yellowish micrites and radiolarian biomicrites (wackestones to packstones). More explicitly, the calcareous beds (Vigla Limestones) of the lower part consist of mudstones-wackestones, biomicrites with foraminifera and radiolaria, and siliceous wackestones and packstones [42]. In the upper part, this formation consists of the Vigla Shale member (also known as “Upper siliceous zone”; [66]) composed by yellow marly or shaly limestones and shales with chert intercalations, and red to green or locally black clay layers. The latter contains the equivalent of the anoxic events of Selli (OAE1a) during the Aptian-Albian, Paquier Evet (OAE1b) of Early Albian age and Bonarelli (OAE2) at the Cenomanian-Turonian boundary in the Ionian zone [12,14,73,74], and extends to Italy and Albania. Vigla Limestones generally feature considerable lateral variations in thickness, mainly in the basin borders where its thickness may reach the double of its average, which is indicative of persistent differential subsidence [34,58,59]. In the internal sub-basin, the Vigla Limestones consist of compact, thick-bedded, often bituminous, dolomitic limestones, with lenses of slightly dolomitized microbreccia and thin cherty intercalated layers or nodules. It is also characterized by the presence of several aptychus in its lower part [59,64]. In Epirus, along the eastern border of the central Ionian zone, phosphatic horizons are intercalated with the uppermost horizons of the Vigla Limestone formation, stratigraphically above the Vigla Shale member. Overall, this formation corresponds to the first post-rift sediments of the Ionian zone [58,59,64].

### 2.2.3. Senonian Limestones

This formation corresponds to thick pelagic strata (1 to 3 m) intercalated with calciturbidites, comprising limestones with fragments of globotruncanids and rudists and fine-grained breccia intervals with limestones and rudist fragments within calcareous cement containing pelagic fauna. Calciturbidites are usually alternated with sub-lithographic pelagic limestones and cherts [34,35]. Overall, this formation corresponds to a period of basinal sedimentation, with significant variations of its lithological characteristics and sedimentary facies from the external (western) to the internal (eastern) parts of the Ionian basin. In the external sub-basin, they have been described as “clastic limestones” [75] containing floatstones, rudstones and rare grainstones and packstones with a micritic matrix, biomicritic intercalations, and rare cherty nodules. In the middle sub-basin, these carbonates are characterized as microclastic, bioclastic or polygenic microbreccias with a micritic matrix (wackestone, packstones), intercalated with (bio)micrites. In the internal sub-basin, the Senonian Limestones are massive, thick bedded microbreccias to breccias containing rudists and coral fragments, with only local appearance of thin-bedded or nodular chert [65,66,76].

### 2.2.4. Paleocene-Eocene Limestones

This formation also known as “Limestones with microbreccia” [75] is characterized by the same sedimentary facies with the underlying formation, with prominent microbreccia derived from the erosion of Cretaceous carbonates from both the Gavrovo (to the east) and Apulian (to the west) platforms. On Late Paleocene and progressively through the Early Eocene, the supply of calciclastic material diminished significantly, especially in the central Ionian Basin. The main depositional facies during the Eocene were platy wackestone and mudstone with Globigerinidae and chert nodules, analogous to those of the Vigla Limestones, but lack continuous siliceous intervals [34].

## 3. Materials and Methods

Six sections (A–F; Figure 2A–E) were sampled every 1 m and studied in terms of their reservoir parameters, paleodeposition environment, and paleogeographic significance.

Section A (Agios Georgios Section) is situated at the entrance of Agios Georgios village (lat: 39°16'14.99" N, lon: 20°50'59.43" E; Figure 2B). This section belongs to the Pantokrator Limestones (Figure 3), with a total length of 50 m, where 50 samples have been collected (Figure 4).

Section B (Perivleptos section) is situated at the north part of Perivleptos village (lat: 39°46'21.90", lon: 20°46'48.34" E; Figure 2C). This section covers parts of Pantokrator Limestones and Vigla Shales (Figure 3). The total length of the section is 20 m, where 20 samples have been collected (Figure 4).

Section C (Vigla Section) is situated at the south part of Asprageli village (lat: 39°48'33.45" N, lon: 20°43'38.73" E; Figure 2D). This section covers partially the Vigla Limestones (Figure 3) with a total length of 20 m, where 20 samples have been collected (Figure 4).

Section D (Koloniati section) is situated at the north part of Koloniati village (lat: 39°34'52.46" N, lon: 20°53'11.41" E; Figure 2E). This section covers the upper part of the Vigla Limestones and the lower part of the Senonian Limestones, which are separated by an unconformity (Figure 3). The total length of the section is 60 m, where 30 samples have been collected every 2 m (Figure 4).

Section E (Asprageli-2 Section) is situated at the north-east part of Asprageli village, near the section C (lat: 39°49'54.00" N, lon: 20°43'58.25" E; Figure 2D). This section covers the Senonian Limestones (Figure 3), with a total length of 10 m, where 10 samples have been collected (Figure 4).

Section F (Asprageli-1 Section) is situated at the north-east part of Asprageli village (lat: 39°45'57.42" N, lon: 20°43'58.25" E; Figure 2D). This section covers the part of Paleocene-Eocene limestones (Figure 3), with a total length of 25 m, where 25 samples have been collected (Figure 4).

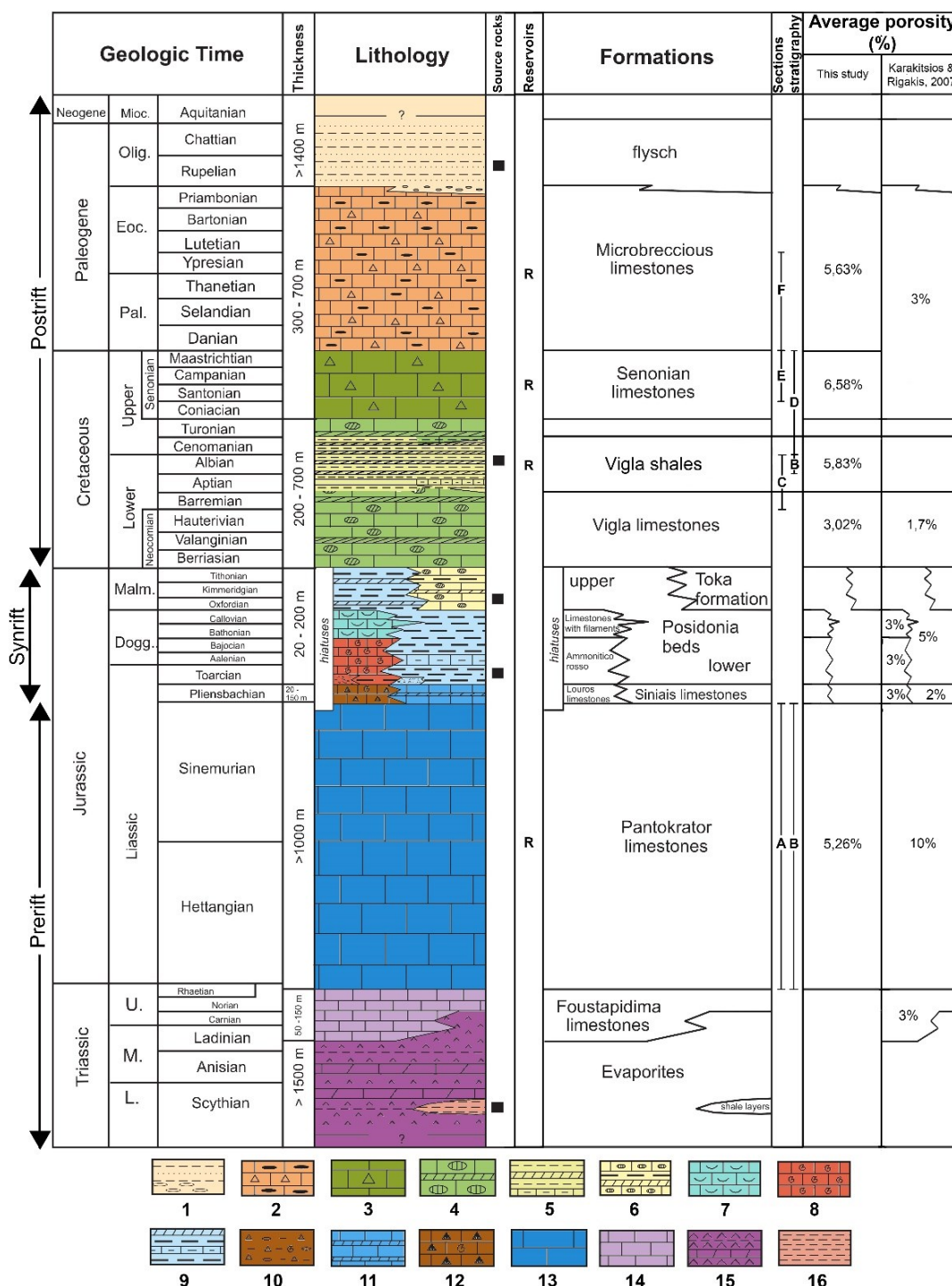


**Figure 3.** Synthetic lithostratigraphic column of the Ionian zone (modified from [34]), along with the correspondence of study sections stratigraphy with Ionian formations and their average porosity values as potential reservoir rocks. The colors in the lithostratigraphic column are consistent with the relevant colors of the International Chronostratigraphic Chart (v2020/01). (1) Shales and sandstones; (2) limestones with rare cherty intercalations, occasionally microbreccious; (3) pelagic limestones with clastic platform elements; (4) pelagic limestones with cherts; (5) cherty beds with shale and marl intercalations; (6) pelagic limestones with cherty nodules and marls; (7) pelagic limestones with bivalves; (8) pelagic, nodular red limestones with ammonites; (9) marly limestones and laminated marls; (10) conglomerates-breccias and marls with ammonites; (11) pelagic limestones with rare cherty intercalations; (12) external platform limestones with brachiopods and small ammonites in upper part; (13) platform limestones; (14) thin-bedded black limestones; (15) evaporites; (16) shales.

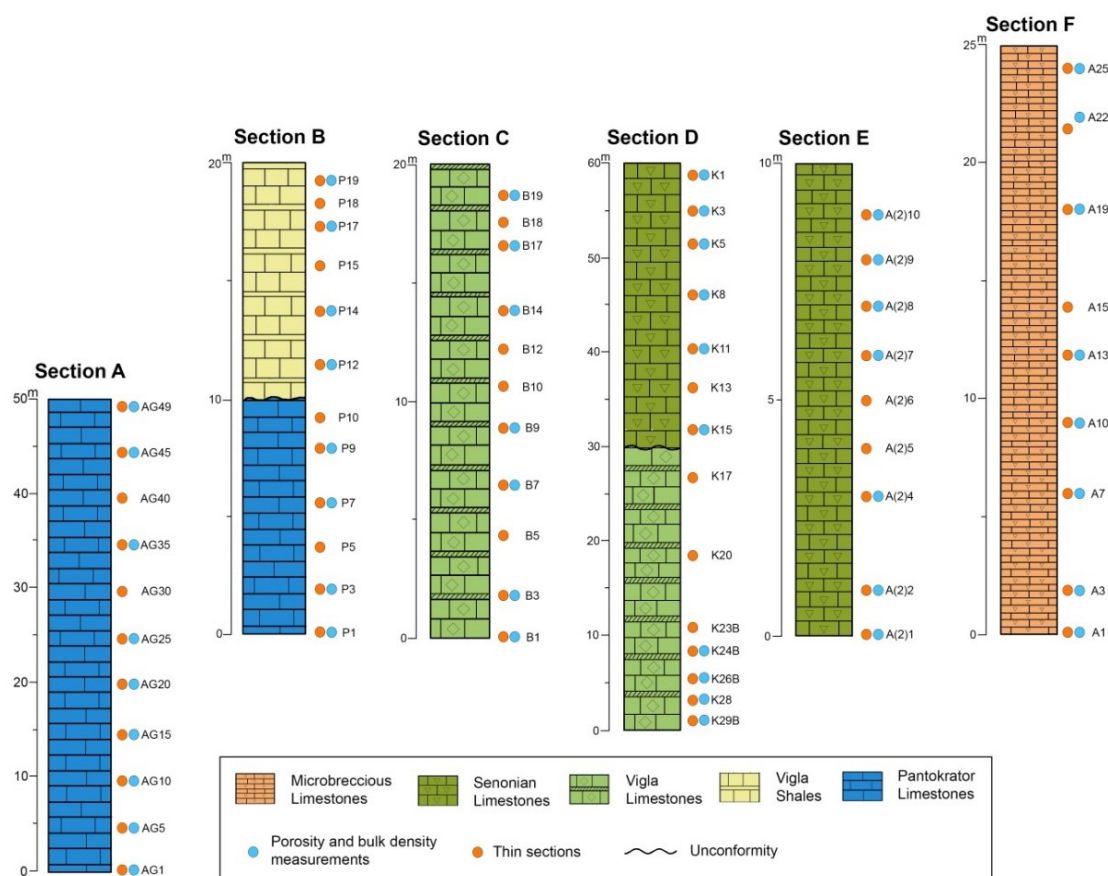


**Figure 4.** Lithology of the 6 study sections in Epirus region. The orange and blue circles at the right of each column represent the sampling intervals for thin sections as well as porosity and bulk density measurements.

The study of the Jurassic to Eocene sediments’ distribution was based on tectonic, stratigraphic, paleontologic, and sedimentologic observations. Depending mostly on outcropping conditions, an average sampling interval of approximately 1 m has been used. An overall number of 150 samples were collected, among which 70 used for sedimentary facies analysis and 50 for measuring porosity and bulk density. Microfacies definition and textural characters analysis of the carbonate rocks, including both biogenic and inorganic dominant components, were done according to carbonate classification schemes of [77], which later modified by [78], based on the Standard Microfacies Types (SMF) in the facies zones (FZ) of the rimmed carbonate platform model. Depositional environments were reconstructed based on the derived sedimentological features and through comparison with additional standard facies reconstructions [79–85]. Therefore, assemblages consisting of several SMF types characterize all depositional environments. Thin sections were prepared in the Historical Geology and Paleontology Laboratory (National and Kapodistrian University of Athens; NKUA), biostratigraphically and sedimentologically studied under a polarized LEICA DM LP microscope, and photos have been performed with OLYMPUS UC30 Microscope Digital Camera. The reservoir potential of these carbonates was also obtained through the examination of porosity and bulk density parameters on representative of each stratigraphic formation samples, with the use of GeoPyc 1360 Envelope Density Analyzer and helium AccuPyc 1330 Pycnometer, respectively, also at NKUA. All measurements were made on dry samples that were previously dried in the oven at 40 °C for 24 h. The petroleum potential information was further compared with existing regional data covering the studied stratigraphic interval. Finally, ArcGIS software was used to visualize the results of the study area, along with additional data known from the literature, outcropped and well data [33,35,42,59,86] expanding the entire Ionian zone within paleogeographic/paleoenvironmental maps for the relevant time interval.

## 4. Results

### 4.1. Description of the Study Sections

Figure 5 illustrates a general view of the studied sections, regarding the Jurassic-Eocene carbonates of the Ionian zone in the study area. Agios Georgios section consists of 50 m of a uniform, largely condensed shallow-water limestone unit (Figure 5a,b) with calcareous algae, benthic foraminifera, and, rarely, brachiopods. The middle part of this succession (samples L15–L20) is recrystallized and slightly dolomitized, a phenomenon that usually occurred during the Jurassic in the Ionian zone. Such Early Jurassic sediments represent the lower part of the carbonate unit in western Greece. The basal 10 m of Perivleptos section contains neritic Pantokrator Limestones, overlain unconformably by reddish and green organic matter-rich shales with thin- to medium-bedded marly limestone interbeds and siliceous lenses, the Vigla Shales (Figure 5c–e).



**Figure 5.** Outcrop photographs of the study sections along with enlargements indicative of their characteristics: (a) General panoramic view of the Agios Georgios section; (b) Early Jurassic Pantokrator Limestones of Agios Georgios section; (c) general panoramic view of Perivleptos section. The red dashed line marks the unconformity between the lower (Pantokrator Limestones) and the

upper (Vigla Shales) part of the section; (d) Pantokrator Limestones of the lower part of Perivleptos section; (e) Vigla Shales of the upper part of Perivleptos section; (f) general panoramic view of Vigla section; (g) enlargement of the Vigla section, showing pelagic limestones and with chert intercalations; (h) general panoramic view of Koloniati section; (i) Vigla Limestones of the lower part of Koloniati section. The red dashed line marks the unconformity between the lower (Vigla Limestones) and the upper (Senonian Limestones) part of the section; (j) Senonian Limestones of the upper part of Koloniati section; (k) enlargement of the Vigla Limestones, showing pelagic limestones intercalated with flattened cherty nodules; (l) general panoramic view of Asprageli-2 section; (m) Senonian Limestones of Asprageli-2 section; (n) general panoramic view of Asprageli-1 section; (o) Paleocene-Eocene microbrecciated limestones of Asprageli-1 section.

The Vigla section, which has a thickness of 20 m, is characterized by typical Vigla formation deposits, such as pelagic limestones interbedded with centimeter- to decimeter-thick radiolarian chert beds (Figure 5f,g). Koloniati section (60 m thickness) consist of Cretaceous deposits of both Vigla and Senonian Limestones formations separated by an unconformity (Figure 5i). The lower half consists of pelagic massive limestones with rare intercalations of chert beds, and spherical, but also flattened, cherty nodules (Figure 5i,k). The siliceous nodules are beige, or light grey to dark grey color. The lithology of the upper half is described as solid, thick-bedded limestones that can be easily separated from the underlain thin-bedded ones (Figure 5j). In the uppermost part of the section brecciated horizons have been observed. Similar microbreccia bioclastic limestones with roudist fragments were observed in the 10 m thick Asprageli-2 section (Figure 5l,m). Finally, at the top of the studied carbonate succession, the 25 m thick Asprageli-1 section consists of grey-light micro- to mesoporous, turbiditic limestones with abundant radiolaria and planktonic foraminifera (Figure 5n,o).

#### 4.2. Sedimentary Facies Analysis

Section A (Agios Georgios Section): The principal lithofacies of this section is boundstone, composed of red algal communities, and less frequent benthic foraminifera within a micritic clotted matrix (Figure 6a,b). Some lime horizons are dolomitized.

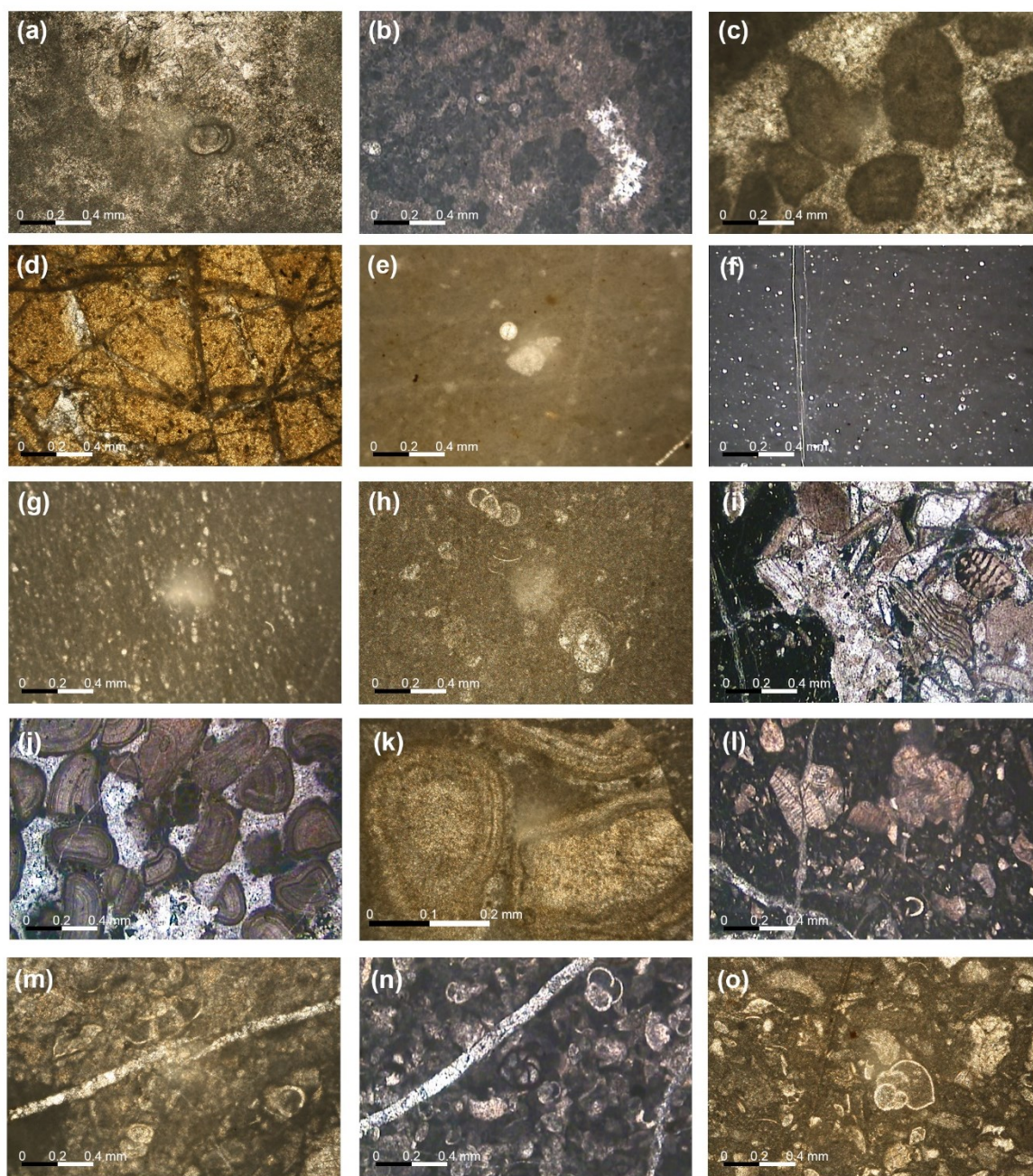


**Figure 6.** Characteristic Early Jurassic to Paleogene microfacies types of Ionian zone (Epirus region, NW Greece). (a,b) Dolomized boundstone with calcareous algae and benthic foraminifera within a micritic clotted matrix (samples AG1, AG15); (c,d) recrystallized grainstone of peloids with signals of dolomitization and fracturing (samples P3, P9); (e) mudstone-wackestone with radiolarian and planktonic foraminifera (sample P19); (f,g) wackestone with radiolarians (samples B1, B10); (h) Pelagic wackestone with radiolarians and planktonic foraminifera (sample K2); (i) Allochthonous bioclastic packstone with medium- and large-sized bioclasts benthics and rudist fragments (sample K5); (j,k) grainstone of ooids with sparitic cement (samples K4, K9); (l) bioclastic packstone of orientated and transported larger benthic foraminifera and rudists (sample A(2)7); (m) Pelagic wackestone-packstone of radiolarian and planktonic foraminifera, among which carenate forms are presented (sample A(2)9); (n,o) packstone with in situ planktonic foraminifera and scattered, transported benthics and mollusks (samples A7, A13).

Section B (Perivleptos section): The lower part of this section is characterized by the lithofacies recrystallized grainstone of peloids with signals of dolomitization and fracturing (Figure 6c,d), while

the upper part consists of mudstone-wackstone with radiolarians and/or planktonic foraminifera (Figure 6e).

Section C (Vigla Section): Section E consists of radiolarian biomicrite wackstone (Figure 6f,g).

Section D (Koloniati section): Within this section biomicrite mudstone-wackstone with planktonic foraminifera (Figure 6h), allochthonous bioclastic packstone with abundant benthic foraminifera (Figure 6i), and ooid lithofacies (Figure 6j,k) were observed.

Section E (Asprageli-2 Section): In Section D, the following two lithofacies have been observed: (i) bioclastic packstone, (Figure 6l), and (ii) biomicrite wackstone-packstone-floatstone with planktonic foraminifera, (Figure 6m).

Section F (Asprageli-1 Section): In Section C a packstone with planktonic foraminifera and some scattered mollusc and benthic foraminifera (Figure 6n,o) has been identified.

Generally, high energy environments such as platform, fore-shoal, and intertidal channel display grain supported textures. On the contrary, in low energy environments such as deep shelf and open marine, mud supported textures developed. In between, medium energy settings include platform slope environments, deposits of which are characterized by significant debris of rudists, algae, porcelaneous benthic foraminifera, and rarely variable shell fragments (bivalves, bryozoans). Grainy or micritic texture also strongly affected porosity, fluid flow, and diagenetic processes.

### 4.3. Biostratigraphic Analysis

Section A (Agios Georgios Section): Calcareous green algae of *Paleodasycladus* sp. and *Paleodasycladus mediterraneus* and *Thaumatoporella parvoovesiculifera*, *Thaumatoporella* sp. build boundstones. Benthic foraminifers are represented by *Textularia* sp., Miliolidae and Ataxophragmiidae.

Section B (Perivleptos section): Benthic foraminifera (e.g., *Glomospira* sp., *Glomospirella* sp., *Globochaete* sp., *Textularia* sp., *Valvulina* sp., Miliolidae, *Clypeina jurassica*, *Protopeneloplis striata*) and fragments of hermatypic corals, calcareous green algae, gastropods, were identified in the lower part of the section and suggest a Hettangian-Sinemurian age. Radiolarians and planktonic foraminifera *Ticinella roberti*, *Biticinella breggiensis*, *Hedbergella delrioensis*, *Hedbergella planispira*, place the upper part of this section to the Middle-Late Albian.

Section C (Vigla Section): Assemblages of small-to-medium-sized morphotypes of *Calpionella alpina* followed by the acme of *Calpionella elliptica* at the basal part of the section suggest an Early Berriasian age, while progressively through the top of the section radiolarians and other planktonics (*Favusella hauerivica*, *Hedbergella sigali*, *Hedbergella dendroensis*) have been further identified. In the upper half of the section the Globigerinelloides “acme” and “eclipse” intervals, characterized by the abundant presence and the lack of representatives of this genus, respectively, show the evolution through the Barremian up to the Albian in the topmost meters of the Vigla Limestones.

Section D (Koloniati section): The lower part of the section assigned to Vigla Formation was characterized by the presence of the planktonic foraminiferal assemblage *Rotalipora appenninica*, *Rotalipora cushmani*, and *Praeglobotruncana gibba* suggesting the early Late Cretaceous and particularly the Cenomanian-Turonian boundary interval. The upper part has a Coniacian-Maastrichtian age and contains the foraminifera *Globotruncana* cf. *arca*, *Globotruncana* cf. *linnei*, *Orbitoides* sp., *Quinqueloculina* sp., *Spiroloculina* sp., *Pseudolituonella* sp., *Cuneolina* sp., Textulariidae, and Miliolidae.

Section E (Asprageli-2 Section): This section cover the Santonian-Maastrichtian time span based on the variable fauna containing mainly Globotruncaniids (e.g., *Globotruncanita stuarti stuatiformis*, *Rugoglobigerina rugosa*, *Globotruncana* cf. *bulloides*, *Globotruncana arca*, *Abathomphalus mayaroensis*, *Contusotruncana* sp.), but also benthic foraminifera (e.g., Miliolidae, *Siderolites* sp., *Cuneolina* sp., *Orbitoides* cf. *media*, *Orbitoides apiculata*), as well as rudist and molusc fragments.

Section F (Asprageli-1 Section): The genera Subbotina, Acarinina, and Morozovella are the dominant groups of Paleocene-Early Eocene assemblages. More explicitly, the lower part of the section contains carbonates enriched on radiolarians and planktonic foraminifera (*Parasubbotina pseudobulloides*, *Acarinina* sp., *Subbotina* sp., *Igorina pussila*, *Chiloguembelina* sp.), which deposited during the Early Paleocene (Selandian). Progressively through the top of the section, the increase of

highly and full body ornamented Morozovellid species (e.g., *Morozovella aequa* and *Morozovella subbotinae*, *Morozovella velascoensis*) and quadrate Acarininids (e.g., *Acarinina wilcoxensis* and *Acarinina pseudotopilensis*) are indicative to the end of the Paleocene and the start of the Eocene (Ypresian).

Overall, the age determination supports the pre-existing results mentioned in the geological maps (Ioannina, Doliana, Pappadai, and Tsepelovo sheets; [87–90]) regarding the Ionian zone rock exposures. Particularly, they confirm the Early Jurassic (Hettangian-Sinemurian) for the Pantokrator Limestones, the Early Cretaceous-early Late Cretaceous (Berriasian-Turonian) for the Vigla Limestones, the early Late Cretaceous (Albian) for the Vigla Shales, the Late Cretaceous (Coniasian-Maastrichtian) for the Senonian Limestones, and the Paleocene/Early Eocene age for the microbreccious limestones respectively.

#### 4.4. Porosity and Bulk Density Measurements

The results of porosity and bulk density measurements of the studied carbonates are listed in Table 1, while the average values per formation in Table 2. With the exception of Vigla Shales, which present the lowest measured bulk density values (2.60–2.63; average 2.62 gr/cm<sup>3</sup>), the bulk density is quite homogeneous for all carbonate samples, ranging from 2.64 to 2.74 gr/cm<sup>3</sup>, with an average of 2.68–2.70 gr/cm<sup>3</sup>, respectively, per study formation (Table 2). On the contrary the total porosity values evaluated with the pycnometer present significant variability between the different sections and stratigraphic formations. In Agios Georgios section porosity values range between 2.31% and 9.71%, with an average value of 4.97% (Table 1). Significant porosity values above the average value for the Jurassic deposits were recorded in some horizons of this unit (samples AG10-20), where the limestones seem to be dolomitized. These values approximate the maximum porosities (~10%) that have been reported for this formation for the entire Ionian zone [33]. The total average porosity for the Pantokrator Limestones, including both Agios Georgios and the lower part of Perivleptos sections, is 5.26% (Table 2).

**Table 1.** Porosity and bulk density measurements displayed from all the study sections.

Section	Formation	Sample ID	Height (m)	Porosity (%)	Bulk Density (g/cm <sup>3</sup> )
Section F (Asprageli-1)	Limestones with breccia	A1	0	9.35	2.64
		A3	2	3.90	2.61
		A7	6	7.38	2.65
		A10	9	8.55	2.68
		A13	12	2.50	2.71
		A19	18	3.46	2.67
		A23	22	4.32	2.72
Section E (Asprageli-2)	Senonian Limestones	A25	24	5.60	2.74
		A(2)1	0	3.31	2.72
		A(2)2	1	4.52	2.72
		A(2)4	3	2.60	2.74
		A(2)7	6	8.64	2.69
		A(2)8	7	9.63	2.73
		A(2)9	8	7.36	2.62
Section D (Koloniati)	Senonian Limestones	A(2)10	9	8.99	2.70
		K1	0	8.88	2.69
		K3	4	9.26	2.68
		K5	8	5.47	2.69
		K8	14	3.86	2.72
		K11	20	6.56	2.72
		K15	26	5.46	2.72
Vigla Limestones	Vigla Limestones	K28	52	1.28	2.67
		K24B	44	2.33	2.69
		K26B	48	3.87	2.69
		K29B	54	5.65	2.69

Section C (Vigla)	Vigla Limestones	B1	0	3.36	2.73
		B3	2	3.86	2.70
		B7	6	1.81	2.71
		B10	9	3.52	2.68
		B14	13	2.45	2.71
		B18	17	2.07	2.73
		B20	19	2.98	2.69
Section B (Perivleptos)	Vigla Shales	Π20	19	6.00	2.63
		Π18	17	8.10	2.60
		Π15	14	5.82	2.62
		Π12	11	3.38	2.61
	Pantokrator Limestones	Π9	8	8.18	2.72
		Π7	6	7.67	2.72
		Π3	2	3.75	2.72
		Π1	0	4.02	2.66
Section A (Agios Georgios)	Pantokrator Limestones	AG1	0	2.49	2.70
		AG5	4	3.55	2.73
		AG10	9	9.71	2.72
		AG15	14	9.62	2.68
		AG20	19	7.56	2.69
		AG25	24	3.28	2.73
		AG35	34	2.31	2.70
AG45	44	3.76	2.65		
AG50	49	2.45	2.66		

**Table 2.** Average porosity and bulk density values per studied formation of the Ionian zone.

Formation	Stratigraphy	Average Porosity (%)	Average Bulk Density (gr/cm <sup>3</sup> )
Limestones with microbreccia	Paleocene/Eocene	5.63	2.68
Senonian calciturbidites	Late Cretaceous	6.50	2.70
Vigla Shales	late Early Cretaceous	5.83	2.62
Vigla Limestones	Early Cretaceous	3.02	2.70
Pantokrator Limestones	Early Jurassic	5.26	2.70

Porosity measurements of the Perivleptos section document steadily high values for both lithostratigraphic members, with quite similar values (3.75–8.18%, average 5.91%; Table 1) for the basal Jurassic interval and the overlying Vigla Shales (3.38–8.10%, average 5.83%; Table 1). On the contrary, the typical Vigla Limestones in both Vigla section and the lower part of Koloniati outcrop display the lowest values ranging between 1.81% and 3.86% (average 2.86%) in the former and 1.28% and 5.65% (average 3.28%) in the latter (Table 1). Overall, the average porosity for Vigla Limestones, taking into account the data from both aforementioned areas, equals to 3.02% (Table 2). The analyzed samples from the upper part of Koloniati section characterized as Senonian Limestones showed steadily high porosity in the range of 3.86% to 9.26% (average 6.58%), especially at the top of this unit, where brecciated limestones with the maximum porosities of about 10% were identified (Table 1). The same range showing the tendency for increased porosity values (2.60–9.63%, average 6.44%; Table 1) was observed in Asprageli-2 section, with the hemipelagic calciturbidites and fractured resedimented microbreccia. The total average porosity measured for this Late Cretaceous carbonate unit is 6.50% (Table 2). The porosity of Asprageli-1 brecciated Paleogene limestones is in the range of 2.50–9.35% (Table 1), with the average of 5.63% (Table 2).

## 5. Discussion

### 5.1. Microfacies Types and Depositional Environments

The main textural and compositional characteristics, as well as the sedimentary features of the distinguished microfacies, are summarized in Table 3, corresponding to different depositional environments or facies zones (FZ) defined by [84,85] (Figure 7). More specifically, the Pantokrator Limestones were classified as boundstone of algae (SMF 7) and bioclastic grainstone (SMF 11) in the Agios Georgios and Perivleptos sections respectively, giving evidence of a depositional environment characterized by a platform, with both intertidal and subtidal environments (FZ5-6). Recrystallization-dolomitization and fracturing of some redeposited carbonate clasts points a subaerial exposure of parts of the platform. Vigla Limestones consist of mudstone-wackestone with radiolarians and planktonic foraminifera (SMF 2-3), characterizing a low energy, relatively deep environment, such as the toe of slope (FZ3) and/or deep shelf (FZ2). Senonian Limestones present a variety of lithofacies, which correspond to environments ranging from the slope to deep shelf. They mostly include in-situ wackestone-packstone with planktonic foraminifera along with microbreccia bioclastic packstone with fragments of shallow water fauna (rudists and benthic foraminifera) (SMF 4), and micrite with transported ooids (SMF 13), which in total represent a medium-to-high-energy environment (e.g., slope), possibly due to the transportation of the sediments within the basin from the platform.

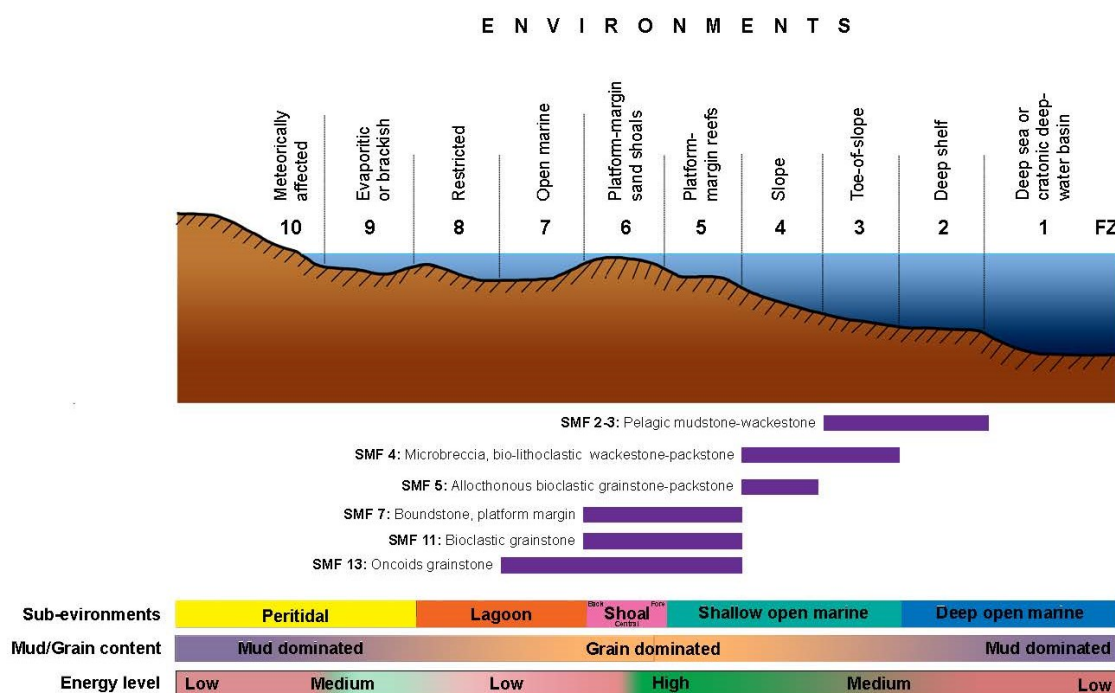


**Figure 7.** Depositional distribution model in the Ionian zone. The sedimentary changes display good correlation with the energy level of environments and facies changes.

The above facies distribution reflects the separation of the deep Ionian Basin into a central topographically-higher area characterized by reduced sedimentation, and two surrounding talus slopes with increased sedimentation [66]. Locally, micritic peloids and dark-gray intraclasts, floating in an overall micritic matrix were also observed within these carbonates. The range of depositional interpretations of these formations includes supratidal settings, vadose-marine inorganic precipitation in inter- and subtidal environments of formation in marine seepage or groundwater springs [85]. Overall, Late Cretaceous calciturbidites suggest relatively deep-slope depositional conditions (FZ3-4). Relatively similar and possibly deeper depositional conditions apply for the

Paleogene biomicritic packstones with radiolaria (mostly at the Early Paleocene) and planktonic foraminifera (through the Eocene) (SMF3), suggesting a basinal environment (FZ2).

**Table 3.** Detailed description of representative thin sections, where sedimentary facies, lithology, formation, age, and the depositional environments of the studied deposits are presented.

Section	Samples	Formation	Lithology	Facies Description	Figures	Depositional Environment	Stratigraphy (Stages)
F: Asprageli-1	A7, A13	Limestones with microbreccia	Hemipelagic calciturbidites with microbreccia	Packstone with in-situ planktonic foraminifera and scattered, benthic foraminifera and mollusks (SMF 3)	Figure 6n,o	Shelf slope (FZ3) to deep shelf (FZ2) (medium energy)	Paleocene to Eocene
E: Asprageli-2	A7, A9	Senonian Limestones	Microbrecciated bioclastic to pelagic turbiditic limestones	(a) Allochthonous bioclastic packstone with rudists and benthic foraminifera (SMF 5), (b) Pelagic wackestone-packstone with radiolarian and planktonic foraminifera (SMF 4-5)	Figure 6l,m	Slope (FZ4) - toe of slope (FZ 3) to deep shelf (FZ 2) (medium energy)	Late Cretaceous (Santonian-Maastrichtian)
D: Koloniati (upper part)	K2, K9, K4, K5	Senonian Limestones	Bioclastic Limestones (often brecciated)	(a) Allochthonous bioclastic packstone to grainstone with rudist fragments and benthic foraminifera (SMF 5), (b) Mudstone-wackestone with planktonic foraminifera (SMF 4-5), (c) Grainstone of ooids with sparite cement (SMF 5)	Figure 6h,i,j,k	Slope (FZ 4) (medium to high energy)	Late Cretaceous (Santonian-Maastrichtian)
C: Vigla, D: Koloniati (lower part)	B1, B10	Vigla Formation	Limestones intercalated with cherts	Wackestone with radiolarians and planktonic foraminifera (SMF 3)	Figure 6f,g	Toe of slope (FZ 3) (low energy)	Early Cretaceous-early Late Cretaceous (Berriasian-Turonian)
B: Perivleptos (upper part)	P19	Vigla Formation	Shales with marly limestone interbeds and siliceous nodules	Mudstone-wackestone with radiolarians and planktonic foraminifera (SMF 3)	Figure 6e	Deep shelf (FZ 2) (low energy)	late Early Cretaceous-early Late Cretaceous (Aptian-Turonian)
B: Perivleptos (lower part)	P3, P9	Pantokrator Limestones	Neritic limestones	Recrystallized grainstone of peloids with lithoclasts (SMF 5). Signals of dolomitization and fracturing	Figure 6c,d	Inner platform with intertidal and subtidal environments (FZ 4) (moderate energy)	Early Jurassic (Hettangian-Sinemurian)
A: Agios Georgios	AG1, AG15	Pantokrator Limestones	Limestones locally dolomitized	Dolomized boundstone with calcareous algae and benthic foraminifera within a micritic clotted matrix (SMF 7)	Figure 6a,b	Platform (FZ 5) (high energy)	Early Jurassic (Hettangian-Sinemurian)

### 5.2. Reservoir Potential of the Early Jurassic to Eocene Carbonate Rocks of the Ionian Zone

Reservoir characterization deals with physical characteristics of the reservoir, including petrophysics (porosity–bulk density and grain density measurements, capillary pressure measurements), fluid properties (e.g., reservoir fluid saturations) and reservoir drive mechanisms [51,91]. Moreover, reservoir quality is defined as the amount of porosity and bulk density in a reservoir and can be a function of many control factors for both carbonates and sandstones [92–94]. In the present study, the reservoir properties, porosity and bulk density, are comparatively examined in the studied sections on a large intra-basin scale in order to assess the quality of carbonate reservoirs of the Ionian zone. Measuring porosity and bulk density of a given reservoir is a direct measure for the storage and flow capacity. Though porosity seems to be a main contributor to the flow capacity, bulk density is mostly controlled by the pore throat distribution [95]. However, they are difficult to predict, since they depend on both initial depositional processes and diagenetic overprinting. Particularly, their complexity in carbonate reservoirs should be attributed to the different interplays, among other factors, of hydrodynamic conditions, carbonate cementation or dissolution, and tectonic setting that form the architecture of the marine setting [96].

The surveyed carbonates showed remarkable average porosities (3.02–6.50%; Table 2) accompanied by even lower bulk densities (2.62–2.70%), and therefore, the quality of the reservoir has been described as poor to fair. Low and homogeneous bulk density values are in good agreement with the literature data for pure calcite rocks [97–99]. Average porosity values are quite variable in the study sections, with a tendency to slightly higher values in section E and upper part of section D both of Senonian age, as well as in the upper part of section B corresponding to the Vigla Shales. On the contrary, the lowest porosity (and bulk density) values were reported for the biomicritic mudstone-wackestone depositional facies with pelagic fauna of Vigla formation. The Pantokrator Limestones present significant porosity and bulk density values only on dolomitized horizons, explaining the significant variability observed into this formation. Generally, this intra-zone original porosity evolution characterized by an increased tendency from the Early Cretaceous pelagic limestones to the Late Cretaceous calciturbidites, which are also slightly more permeable, is consistent with previous findings in the Ionian zone of NW Greece [33,100,101]. Particularly, the overall evolution in the study area display a quite variable average porosity pattern, characterized mostly by low to moderate values (~3–7%), while some high individual values around 10% also recorded. The levels with such a sudden porosity increase may be related to burial diagenesis and dolomitization, which increase the reservoir quality to good.

Factors related to sequence architecture, including the occurrence of intervals with clay laminations (e.g., Vigla Shales; promoting chemical compaction and associated cementation) and the distribution of early dolomitization (promoting porosity preservation during burial), generally increases secondary fracture porosity. A higher increase of porous within the marly limestones of Vigla Shales formation than in Senonian calciturbidites, could be caused due to fracturing due to the nodule's development, in the manner described by [43]. Intracrystalline porosity could be also developed within dolomitized intervals and therefore some breccia limestones may form potential reservoirs. Especially for the Ionian zone, it is documented that the dolomitization front has changed through time [33]. In the internal and external parts of the Ionian zone, dolomitization continued well into the Cretaceous, whilst in the central part, it did not continue after the Middle Jurassic. However, it is worth noting that the low porosity and bulk density identified within the study formations could either imply high fluid pressures or fluid migration through permeable “fracture conduits” in the vicinity of fault zones. The observed porosity values correspond to microporosity that does not take into consideration the fracture porosity related to thrusts which considerably increases the carbonate reservoir quality. Some of the porosity variations observed in this study may due to the vicinity/distance of the samples with the tectonic zones. In any case, distribution of Ionian tectonic zones is related to the prevailing tectonic style of the Ionian zone, which is a combination of thick- and thin-skinned deformation [33]. The elucidation of the predominance of tectonic style has not been

achieved to date, due to the fact that deep seismic surveillance is hindered by the subsurface Ionian evaporites [34,58,70,71].

The incorporation of the depositional with the carbonate reservoir quality data indicate that there is not a clear view for the reservoir quality that can be associated with a specific depositional environment. Generally, in western Greece, most of the fair to good potential reservoirs are deposited in shallow to restricted platforms (e.g., Gavrovo platform carbonates close to its transition to the Ionian zone, in the thrust sheets of Ionian and pre-Apulian zones) [33,34,40]. In the Ionian zone, similar medium to high energy environments, such as tidal domains, reef barriers, and slopes were recorded during Jurassic (e.g., Pantokrator Limestones, Posidonia beds) and Late Cretaceous to Paleocene/Eocene (e.g., Limestones with microbreccia), respectively [35,40]. However, Jurassic studied sediments do not contain any proven reservoirs with the most significant porosities to be associated with the development of fracture and/or diagenetic zones. This study shows that deeper depositional (deep marine basinal and/or slope) environments can also be associated with the deposition of good potential reservoirs. On this regard, potential reservoir rocks within the Ionian zone further include the upper part of pelagic Vigla Limestones, Senonian Limestones, and the microbrecciated intervals of the Paleocene/Eocene limestones, all presented very good porosity values up to 10%.

### 5.3. Paleogeographic Analysis of the Ionian Zone

In Epirus area only the Jurassic to Eocene carbonate succession occurs. The carbonate platform sediments begin at the base with thick-bedded neritic Jurassic Pantokrator Limestones, which feature remarkable facies homogeneity, indicating that an extensive shallow sea was spread all over the study area during that time. In Perivleptos and Agios Georgios sections, this facies association is mostly represented by biolithitic boundstones and biosparite grainstones with calcareous algae and benthonic foraminifera, implying a carbonate margin platform with both intertidal and subtidal environments (Figure 8A). These extensive platforms are developed until the Hettangian–Pliensbachian age, when the overlying synrift sequence begins. Pliensbachian Siniais Limestones correspond to the general deepening of the Ionian Basin. The structural differentiation that followed caused the fragmentation of the initial basin into smaller paleogeographic units with half–graben geometry. This is recorded in the abruptly changing thickness of the synrift formations that take the form of syn-sedimentary wedges [34]. In the deeper parts of the half grabens, these wedges include complete Toarcian-Tithonian successions, whereas in the shallower parts of the half grabens, the successions are interrupted by unconformities. However, this topmost part of the Jurassic is not recorded in the studied sections. In Koloniati section, there is an unconformity between the base of the Vigla Shales and the topmost horizons of the underlying Pantokrator formation, which marks a period of uplift and erosion at the beginning of the Toarcian. This led to occasional karstification of Pantokrator Limestones.

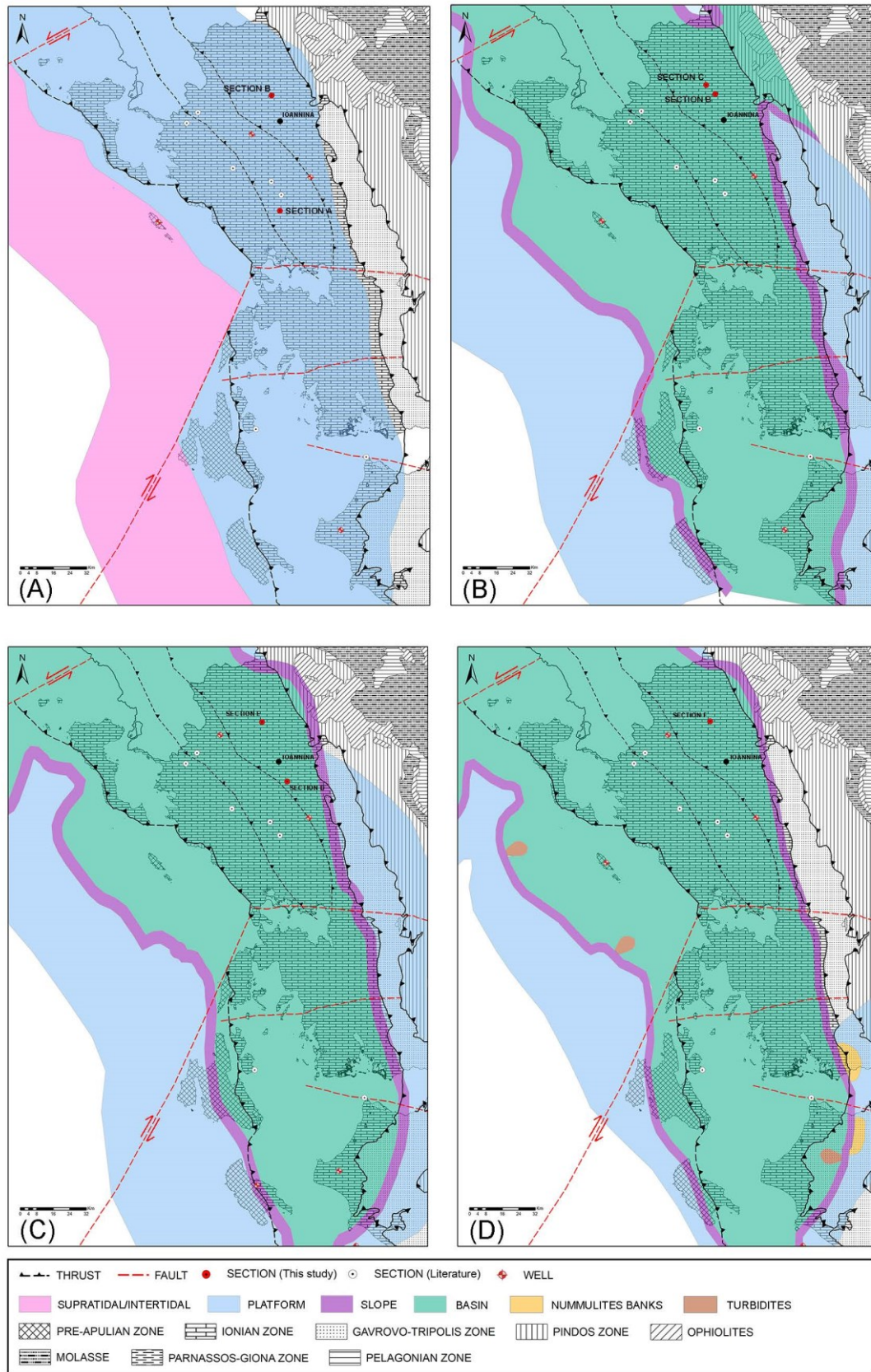


**Figure 8.** Paleo-environmental map of the study area during the (A) Early Jurassic, (B) Early Cretaceous, (C) Late Cretaceous, and (D) Paleocene-Eocene based on outcropped- (red circles from this study and white ones from the literature) and well-data (white-red symbols) [33,35,42,59,86].

The post-rift sequence begins with the pelagic Vigla Limestones, whose deposition was synchronous throughout the Ionian Basin, beginning in the Early Berriasian [73,102]. The basal sequence of the Vigla limestones, consisted of thin layered, sub-lithographic, pelagic limestones, with abundant radiolarian and frequent cherty beds enriched with radiolarian, is related to the Early Cretaceous subsidence caused deepening in the entire basin (Figure 8B). Towards the upper part of this formation, chert layers become more abundant, containing intercalations of green, red, and locally black shales, named as the “Vigla Shales” member, indicative of basinal sedimentation. The microfacies analysis of the Koloniati (lower part) and Vigla sections suggest that these carbonate sediments represent a low energy, relatively deep environment, like the toe of slope and the deep shelf of the basin. Apart from the halokinetic movements, which probably caused the variation in thickness of Vigla Limestones [34] from the western (external) to the eastern (internal) parts of the basin, the pelagic depositional conditions persisted until the Late Eocene, when flysch sedimentation began.

During the Late Cretaceous, the Senonian Limestones formation consisted of hemipelagic calciturbidites and resedimented microbreccia, reflect similar deep marine slope environments. In particular, sedimentary facies analysis of the Koloniati (upper part) and Asprageli-2 samples suggests that they were deposited in a deep-water toe of slope and platform margin environment, respectively, where microbrecciated carbonates were transported and accumulated (Figure 8C). The allochthonous bioclastic material identified in the analysed samples consists mainly of rudist (typical reef builder) fragments and benthic foraminifera (e.g., forereef dweller *Orbitoides*; [103] and/or inner platform taxa *Cuneolina*, Textulariids and Miliolids; [85,103,104]), originated and transported from a nearby shallow shelf environment (e.g., platform or reef). Such shelf margins of the nearby pre-Apulian and Gavrovo platforms [75] and/or internally to the Ionian basin [101] were characterized by high productivity of such skeletal material, transported and redeposited in the deeper parts of the Ionian basin [34]. These bioclasts are also accompanied by pelagic Globotruncanids and radiolarian specimens observed in the in situ micritic matrix. Moreover, ooid lithofacies and some reworked lithoclasts observed in the upper part of the Koloniati Senonian Limestones indicate shallow-water conditions that were exposed during the uppermost interval of the Cretaceous (Maastrichtian). This is further reinforced by extensional tectonics, while possible sea level effects cannot be ruled-out and could also be related to the eustatic sea level low-stand (~150 m sea-level drop) that took place between the Late Cretaceous and the Paleocene [105,106]. Our paleoenvironmental observations from the Late Cretaceous interval in Epirus fully agree with recent sedimentary findings of [42] for the Araxos area (internal Ionian zone), as well as with the previous literature [34,35,75] for the entire Ionian zone. Overall, the facies distribution of the Senonian reflects the separation of the Ionian Basin into a central area (middle and outer part of the Ionian Zone) characterized by deeper water sedimentation and two surrounding talus slopes, issued from western Gavrovo platform and western Apulian platforms. Both platforms provided the clastic carbonate material that was transported by turbidity currents into the Ionian Basin.

The study of the Asprageli-1 samples provides evidence that the supply of clastic material due to tectonics diminished significantly during the Paleocene/Eocene. However, despite the reduced tectonic activity during that time, the slumping of platform edge sediments produced turbidity currents resulting to the deposition of Limestones with microbreccia and calciturbidites. The main depositional facies of platy mudstone-wackestone with Globigerinidae, Globorotaliidae and rare siliceous nodules, analogous to those of the Vigla Limestones, imply that the depositional environments during that period did not change significantly from the Late Cretaceous (Figure 8D). The greatest thicknesses of the Eocene units can be found in the marginal parts of the Ionian Zone, where the microbreccias are more frequent.

## 6. Conclusions

The Ionian zone consists of a heterogeneous multi-layered calciclastic reservoir in Epirus region (western Greece). The identified carbonate formations display various facies ranging in a full spectrum of depositional conditions, from shallow platforms (reefs) to slope (platform margin)

environments, even to the open marine settings, with different lithologies, sedimentary features, energy conditions, and diagenetic overprints. This heterogeneity also explains the rock petrophysical/geomechanical variation of these carbonate rocks. The Early Jurassic limestones (biolithites boundstone) do not contain any proven reservoirs due to relatively low porosities, with the exception of the microcrystallized or dolomited horizons, which increase the reservoir quality in a local scale. The Early Cretaceous limestones and cherts (biomicrites mudstone-wackestone) of Vigla formation has been described as the poorest of the studied carbonates, in terms of their reservoir potential. On the contrary, the Late Cretaceous (Senonian Limestones) and the Paleocene/Eocene carbonate units can be considered the primary target for oil/gas exploration in the study area, since they contain calciturbidites deposited mainly in the slope (bioclastic packstone-rudstone with rudist fragments and benthic foraminifera) and the deep shelf (planktonic foraminiferal biomicrites mudstone-wackestone). The highest porosity values recorded in those carbonates may be further associated with the development of fracture networks and/or diagenetic zones. Overall, the results of this study may have implication for reservoir- and/or source-rock-geologists and diagenetic modelling approaches in the presented area and elsewhere within the eastern Mediterranean Sea [42,86,100,101,107,108], implying that sample specific analyses or a very well understood regional diagenetic framework are required for accurate prediction of reservoir quality.

**Author Contributions:** Conceptualization, G.K., L.M.; methodology, G.K., L.M.; software, L.M., G.K.; validation, G.K., L.M.; formal analysis, G.K., L.M.; investigation, G.K., L.M., V.K., A.A.; resources, L.M., V.K.; data curation, G.K., L.M., V.K., A.A.; writing—original draft preparation, G.K.; writing—review and editing, G.K., L.M., V.K., A.A.; visualization, G.K., L.M.; supervision, V.K., A.A.; project administration V.K., A.A.; funding acquisition, L.M., V.K. All authors have read and agreed to the published version of the manuscript.

**Funding:** This research received no external funding.

**Acknowledgments:** The authors are grateful to Andreas Kostis for his significant contribution to the fieldwork. Professors Jean-Jacques Cornée and Fotini Pomoni-Papaioannou are warmly thanked for her kind assistance during the sedimentary facies analysis and her constructive suggestions regarding the interpreted depositional paleoenvironments. Four anonymous reviewers are deeply acknowledged for useful and constructive comments on the manuscript, and Victoria Li (Assistant Editor) is also thanked for her editorial handling.

**Conflicts of Interest:** The authors declare no conflict of interest.

## References

1. Morse, J.W.; Mackenzie, F.T. *Geochemistry of Sedimentary Carbonates*; Elsevier Science: Oxford, UK, 1990; Volume 48.
2. Schlager, W.; Philip, J. Cretaceous Carbonate Platforms. In *Cretaceous Resources, Events and Rhythms*; Ginsburg, R.N., Beaudoin, B., Eds.; NATO ASI Series (Series C: Mathematical and Physical Sciences); Springer: Dordrecht, The Netherlands, 1990; Volume 304.
3. Bruckschen, P.; Oesmann, S.; Veizer, J. Isotope stratigraphy of the European Carboniferous: Proxy signals for ocean chemistry, climate and tectonics. *Chem. Geol.* **1999**, *161*, 127–163.
4. Erba, E.; Bartolini, A.; Larson, R.L. Valanginian Weissert oceanic anoxic event. *Geology* **2004**, *32*, 149–152.
5. Volery, C.; Davaud, E.; Foubert, A.; Caline, B. Shallow-marine microporous carbonate reservoir rocks in the Middle East: Relationship with seawater Mg/Ca ratio and eustatic sea level. *J. Pet. Geol.* **2009**, *32*, 313–325.
6. Caruso, A.; Pierre, C.; Blanc-Valleron, M.-M.; Rouchy, J.M. Carbonate deposition and diagenesis in evaporitic environments: The evaporative and sulphurbearing limestones during the settlement of the Messinian salinity crisis in Sicily and Calabria. *Palaeogeogr. Palaeoclimatol. Palaeoecol.* **2015**, *429*, 136–162.
7. Kontakiotis, G.; Karakitsios, V.; Mortyn, P.G.; Antonarakou, A.; Drinia, H.; Anastasakis, G.; Agiadi, K.; Kafousia, N.; De Rafelis, M. New insights into the early Pliocene hydrographic dynamics and their relationship to the climatic evolution of the Mediterranean Sea. *Palaeogeogr. Palaeoclimatol. Palaeoecol.* **2016**, *459*, 348–364, doi:10.1016/j.palaeo.2016.07.025.
8. Kontakiotis, G.; Besiou, E.; Antonarakou, A.; Zarkogiannis, S.D.; Kostis, A.; Mortyn, P.G.; Moissette, P.; Cornée, J.-J.; Schulbert, C.; Drinia, H.; et al. Decoding sea surface and paleoclimate conditions in the eastern

- Mediterranean over the Tortonian-Messinian Transition. *Palaeogeogr. Palaeoclimatol. Palaeoecol.* **2019**, *534*, 109312, doi:10.1016/j.palaeo.2019.109312.
9. Coccioni, R.; Sideri, M.; Frontalini, F.; Montanari, A. The *Rotalipora cushmani* extinction at Gubbio (Italy): Planktonic foraminiferal testimonial of the onset of the Caribbean large igneous province emplacement? *Geol. Soc. Am. Spec. Pap.* **2016**, *524*, 79–96.
  10. Ferraro, S.; Coccioni, R.; Sabatino, N.; Del Core, M.; Sprovieri, M. Morphometric response of late Aptian planktonic foraminiferal communities to environmental changes: A case study of *Paraticinella rohri* at Poggio le Guaine (central Italy). *Palaeogeogr. Palaeoclimatol. Palaeoecol.* **2020**, *538*, 109384, doi:10.1016/j.palaeo.2019.109384.
  11. Jenkyns, H. Cretaceous anoxic events: From continent to oceans. *J. Geol. Soc. London* **1980**, *137*, 171–188.
  12. Tsikos, H.; Karakitsios, V.; Van Breugel, Y.; Walsworth-Bell, B.; Bombardiere, L.; Petrizzo, M.; Sinninghe Damste, J.S.; Schouten, S.; Erba, E.; Premoli-Silva, I.; et al. Organic-carbon deposition in the Cretaceous of the Ionian Basin, NW Greece: The Paquier Event (OAE 1b) revisited. *Geol. Mag.* **2004**, *141*, 401–416, doi:10.1017/S0016756804009409.
  13. Coccioni, R.; Luciani, V.; Marsili, A. Cretaceous oceanic anoxic events and radially elongated chambered planktonic foraminifera: Paleocological and paleoceanographic implications. *Palaeogeogr. Palaeoclimatol. Palaeoecol.* **2006**, *235*, 66–92, doi:10.1016/j.palaeo.2005.09.024.
  14. Karakitsios, V.; Tsikos, H.; Van Breugel, Y.; Koletti, L.; Sinninghe Damste, J.S.; Jenkyns, H.C. First evidence for the Cenomanian-Turonian oceanic anoxic event (OAE2 or “Bonarelli” event) from the Ionian zone, western continental Greece. *Int. J. Earth Sci.* **2007**, *96*, 343–352, doi:10.1007/s00531-006-0096-4.
  15. Karakitsios, V.; Tzortzaki, E.; Giraud, F.; Pasadakis, N. First evidence for the early Aptian Oceanic Anoxic Event (OAE1a) from the Western margin of the Pindos Ocean (NW Greece). *Geobios* **2018**, *51*, 187–210, doi:10.1016/j.geobios.2018.04.006.
  16. Graziano, R. Sedimentology, biostratigraphy and event stratigraphy of the Early Aptian Oceanic Anoxic Event (OAE1A) in the Apulia Carbonate Platform Margin-Ionian Basin System (Gargano Promontory, southern Italy). *Cretac. Res.* **2013**, *39*, 78–111.
  17. Kuhnt, W.; Holbourn, A.; Moullade, M. Transient global cooling at the onset of early Aptian oceanic anoxic event (OAE) 1a. *Geology* **2011**, *39*, 323–326.
  18. Premoli-Silva, I.; Sliter, W.V. Cretaceous planktonic foraminiferal biostratigraphy and evolutionary trends from the Bottaccione section, Gubbio, Italy. *Palaeontogr. Ital.* **1995**, *82*, 1–89.
  19. Premoli-Silva, I.; Erba, E.; Salvini, G.; Verga, D.; Locatelli, C. Biotic changes in Cretaceous anoxic events. *J. Foramin. Res.* **1999**, *29*, 352–370.
  20. Leckie, R.M.; Bralower, T.J.; Cashman, R. Oceanic anoxic events and plankton evolution: Biotic response to tectonic forcing during the mid-Cretaceous. *Paleoceanography* **2002**, *17*, 13–29.
  21. Coccioni, R.; Luciani, V. Planktonic foraminifera across the Bonarelli Event (OAE2, latest Cenomanian): The Italian record. *Palaeogeogr. Palaeoclimatol. Palaeoecol.* **2005**, *224*, 167–185, doi:10.1016/j.palaeo.2005.03.039.
  22. Coccioni, R.; Luciani, V. *Guembelitra irregularis* bloom at the K-T boundary: Morphological abnormalities induced by impact related extreme environmental stress? In *Biological Processes Associated with Impact Events: Impact Studies*; Cockell, C., Koeberl, C., Gilmour, I., Eds.; Springer: Heidelberg, Germany, 2006; Volume 8, pp. 179–196, doi:10.1007/3-540-25736-5\_8.
  23. Pomoni-Papaioannou, F.; Photiades, A. Chlorozoan vs. foramol carbonate sedimentary systems in an Upper Jurassic-Cretaceous Pelagonian margin in Rhodiani area (West Macedonia, Greece). *Boll. Soc. Geol. It. (Ital. J. Geosci.)* **2007**, *126*, 172, 32/05–130.
  24. Simone, L.; Carannante, G. Peri-Tethyan Cretaceous shallow-water carbonate systems: Sedimentary patterns and lithofacies. *Geoacta* **2008**, *1*, 193–216.
  25. Simone, L.; Bravi, S.; Carannante, G.; Masucci, I.; Pomoni-Papaioannou, F. Arid versus wet climatic evidence in the “middle Cretaceous” calcareous successions of the Southern Apennines (Italy). *Cretac. Res.* **2012**, *36*, 6–23, doi:10.1016/j.cretres.2012.01.005.
  26. Bernoulli, D.; Jenkyns, H.C. Alpine, Mediterranean, and Central Atlantic Mesozoic facies in relation to the early evolution of the Tethys. In *Modern and Ancient Geosynclinal Sedimentation*; Dott, R.H., Shaver, R.H., Eds.; SEPM Special Publications: Tulsa, Oklahoma, USA, 1974; Volume 19, pp. 129–160.
  27. Philip, J.; Masse, J.P.; Camoin, G. Tethyan carbonate platforms. In *The Ocean Basins and Margins*; Nairn, A.E.M., Ricou, L.E., Vrielynck, B., Dercourt, J., Eds.; The Tethys Ocean Plenum Press: New York, NY, USA, 1995; Volume 8, pp. 239–265.

28. Dercourt, J.; Gaetani, M.; Vrielynck, B.; Barrier, E.; Biju-Duval, B.; Brunet, M.F.; Cadet, J.P.; Crasquin, S.; Sandulescu, M. *Atlas PeriTethys, Palaeogeographical Maps*; CCGM/CGMW: Paris, France, 2000; p. 269.
29. Kiessling, W.; Flügel, E.; Golonka, J. Patterns of Phanerozoic carbonate platform sedimentation. *Lethaia* **2003**, *36*, 195–225.
30. Bernoulli, D. Mesozoic-Tertiary carbonate platforms, slopes and basins of the external Apennines and Sicily. In *Anatomy of an Orogen: The Apennines and Adjacent Mediterranean Basins*; Vai, G.B., Martini, I.P., Eds.; Kluwer Academic Publishers: Great Britain, 2001; pp. 307–326.
31. Vlahović, I.; Tislar, J.; Velić, I.; Matićec, D. Evolution of the Adriatic Carbonate Platform: Palaeogeography, main events and depositional dynamics. *Palaeogeogr. Palaeoclimatol. Palaeoecol.* **2005**, *220*, 333–360.
32. Korbar, T. Orogenic evolution of the external Dinarides in the NE Adriatic region: A model constrained by tectonostratigraphy of Upper Cretaceous to Paleogene carbonates. *Earth-Sci. Rev.* **2009**, *96*, 296–312.
33. Karakitsios, V.; Rigakis, N. Evolution and petroleum potential of western Greece: *J. Petr. Geol.* **2007**, *30*, 197–218.
34. Karakitsios, V. Western Greece and Ionian Petroleum systems. *AAPG Bull.* **2013**, *97*, 1567–1595.
35. Zelilidis, A.; Maravelis, A.G.; Tserolas, P.; Konstantopoulos, P.A. An overview of the petroleum systems in the Ionian Zone, onshore NW Greece and Albania. *J. Petr. Geol.* **2015**, *38*, 331–348.
36. Cazzola, C.; Soudet, H.J. Facies and Reservoir Characterization of Cretaceous-Eocene Turbidites in the Northern Adriatic. In *Accumulation and Production of Europe's Hydrocarbons III Generation*; Spencer, A.M., Ed.; Special Publication of the European Association of Petroleum Geoscientists; Springer: Berlin, Heidelberg, Germany, 1993; Volume 3.
37. Cazzini, F.; Dal Zotto, O.; Fantoni, R.; Ghielmi, M.; Ronchi, P.; Scotti, P. Oil and gas in the Adriatic foreland, Italy. *J. Petr. Geol.* **2015**, *38*, 255–279.
38. Velaj, T.; Davison, I.; Serjani, A.; Alsop, I. Thrust tectonics and the role of evaporites in the Ionian Zone of the Albanides. *AAPG Bull.* **1999**, *83*, 1408–1425.
39. Van Geet, M.; Swennen, R.; Durmishi, C.; Roure, F.; Muchez, Ph. Paragenesis of Cretaceous to Eocene carbonate reservoirs in the Ionian fold and thrust belt (Albania): Relation between tectonism and fluid flow. *Sedimentology* **2002**, *49*, 696–718.
40. Zelilidis, A.; Piper, D.J.W.; Vakalas, J.; Avramidis, P.; Getsos, K. Oil and gas plays in Albania: Do equivalent plays exist in Greece? *J. Petr. Geol.* **2003**, *26*, 29–48.
41. Casabianca, D.; Bosence, D.; Beckett, D. Reservoir potential of Cretaceous platform-margin breccias, central Italian Apennines. *J. Petr. Geol.* **2002**, *25*, 179–202.
42. Bourli, N.; Pantopoulos, G.; Maravelis, A.G.; Zoumpoulis, E.; Iliopoulos, G.; Pomoni-Papaioannou, F.; Kostopoulou, S.; Zelilidis, A. Late Cretaceous to early Eocene geological history of the eastern Ionian Basin, southwestern Greece: A sedimentological approach. *Cretac. Res.* **2019**, *98*, 47–71, doi:10.1016/j.cretres.2019.01.026.
43. Spence, G.H.; Finch, E. Influences of nodular chert rhythmites on natural fracture networks in carbonates: An outcrop and two-dimensional discrete element modelling study. In *Advances in the Study of Fractured Reservoirs*; Spence, G.H., Redfern, J., Aguilera, R., Bevan, T.G., Cosgrove, J.W., Couples, G.D., Daniel, J.M., Eds.; Geological Society, London, Special Publications: London, UK, 2015; Volume 374, pp. 211–249.
44. Coniglio, M.; Dix, G.R. Carbonate slopes. In *Facies Models*; Walker, R.G., James, N.P., Eds.; Geol. Assoc. St. Johns, NL, Canada, 1992; p. 409.
45. Anselmetti, F.S.; Eberli, G.P.; Bernoulli, D. Seismic modeling of a carbonate platform margin (Montagna della Maiella, Italy): Variations in seismic facies and implications for sequence stratigraphy. *Carbonate Seismol.* **1997**, *6*, 373–406.
46. Cilon, A.; Baud, P.; Tondi, E.; Agosta, F.; Vinciguerra, S.; Rustichelli, A.; Spiers, C.J. Deformation bands in porous carbonate grainstones: Field and laboratory observations. *J. Struct. Geol.* **2012**, *45*, 137–157, doi:10.1016/j.jsg.2012.04.012.
47. Cilon, A.; Faulkner, D.R.; Tondi, E.; Agosta, F.; Mancini, L.; Rustichelli, A.; Baud, P.; Vinciguerra, S. The effects of rock heterogeneity on compaction localization in porous carbonates. *J. Struct. Geol.* **2014**, *67*, 75–93, doi:10.1016/j.jsg.2014.07.008.
48. Eberli, G.P.; Baechle, G.T.; Anselmetti, F.S.; Incze, M.L. Factors controlling elastic properties in carbonate sediments and rocks. *Lead. Edge* **2003**, *22*, 654–660, doi:10.1190/1.1599691.

49. Rustichelli, A.; Torrieri, S.; Tondi, E.; Laurita, S.; Strauss, C.; Agosta, F.; Balsamo, F. Fracture characteristics in Cretaceous platform and overlying ramp carbonates: An outcrop study from Maiella Mountain (central Italy). *Mar. Pet. Geol.* **2016**, *76*, 68–87, doi:10.1016/j.marpetgeo.2016.05.020.
50. Trippetta, F.; Carpenter, B.M.; Mollo, S.; Scuderi, M.M.; Scarlato, P.; Colletini, C. Physical and transport property variations within carbonate-bearing fault zones: Insights from the Monte Maggio fault (Central Italy). *Geochem. Geophys. Geosyst.* **2017**, *18*, 4027–4042, doi:10.1002/2017GC007097.
51. Trippetta, F.; Ruggieri, R.; Brandano, M.; Giorgetti, C. Petrophysical properties of heavy oil-bearing carbonate rocks and their implications on petroleum system evolution: Insights from the Majella Massif. *Mar. Pet. Geol.* **2020**, *111*, 350–362, doi:10.1016/j.marpetgeo.2019.08.035.
52. Fabricius, I.L.; Røgen, B.; Gommesen, L. How depositional texture and diagenesis control petrophysical and elastic properties of samples from five North Sea chalk fields. *Petrol. Geosci.* **2007**, *13*, 81–95, doi:10.1144/1354-079306-707.
53. Fabricius, I.; Bächle, G.; Eberli, G. Elastic moduli of dry and water-saturated carbonates-effect of depositional texture, porosity, and permeability. *Geophysics* **2010**, *75*, N65–N78, doi:10.1190/1.3374690.
54. Fitch, P.J.R.; Lovell, M.A.; Davies, S.J.; Pritchard, T.; Harvey, P.K. An integrated and quantitative approach to petrophysical heterogeneity. *Mar. Petrol. Geol.* **2015**, *63*, 82–96, doi:10.1016/j.marpetgeo.2015.02.014.
55. Fjaer, E.H.; Raaen, A.M.; Risnes, R. *Petroleum Related Rock Mechanics*; Elsevier, Science: Amsterdam, Netherlands, 1992; p. 514.
56. Mateus, J.; Saavedra, N.; Carrillo, Z.C.; Mateus, D. Correlation development between indentation parameters and uniaxial compressive strength for Colombian sandstones. *CT&F—Ciencia, Tecnol. Y Futur.* **2007**, *3*, 125–136.
57. Garcia, R.A.; Saavedra, N.F.; Calderon-Carrillo, Z.; Mateus, D. Development of experimental correlations between indentation parameters and unconfined compressive strength (UCS) values in shale samples. *CT&F-Ciencia Tecnol. Futur.* **2008**, *3*, 61–81.
58. Karakitsios, V. The influence of pre-existing structure and halokinesis on organic matter preservation and thrust system evolution in the Ionian basin, northwestern Greece. *AAPG Bull.* **1995**, *79*, 960–980.
59. Karakitsios, V. Ouverture et inversion tectonique du bassin Ionien (Epire, Grèce). *Ann. Géol. Pays Hellén.* **1992**, *35*, 185–318.
60. Doutsos, T.; Koukouvelas, I.; Xypolias, P. A new orogenic model for the External Hellenides. In *Tectonic Evolution of the Eastern Mediterranean Regions*; Robertson, A.H.F., Mountrakis, D., Brun, J.-P., Eds.; Geological Society, London, Special Publications: London, UK, 2006; pp. 507–520.
61. Maravelis, A.; Makrodimitras, G.; Zelilidis, A. Hydrocarbon prospectivity in the Apulian platform and Ionian zone, in relation to strike-slip fault zones, foreland and back-thrust basins of Ionian thrust, in Greece. *Oil Gas Europ. Mag.* **2012**, *38*, 64–89.
62. Konstantopoulos, P.A.; Zelilidis, A. Provenance analysis of Eocene-Oligocene turbidite deposits in Pindos Foreland Basin, fold and thrust belt of SW Greece: Constraints from framework petrography and bulk-rock geochemistry. *Arab. J. Geosci.* **2013**, *6*, 4671–4700.
63. Konstantopoulos, P.A.; Maravelis, A.; Zelilidis, A. The implication of transfer faults in foreland basin evolution. Application on Pindos Foreland Basin, West Peloponnesus, Greece. *Terra Nova* **2013**, *25*, 323–336.
64. Karakitsios, V. Chronologie et Géométrie de L’ouverture d’un Bassin et de Son Inversion Tectonique: Le Bassin Ionien (Epire, Grèce). Ph.D. Thesis, University of Pierre and Marie Curie, Paris, France, 1990, p. 310.
65. Aubouin, J. Contribution à l’étude géologique de la Grèce septentrionale: Le confins de l’Epire et de la Thessalie. *Ann. Geol. Des. Pays Hell.* **1959**, *10*, 1–483.
66. IGRS-IFP (Institut de Géologie et Recherches du Sous-sol Institut Français du Pétrole). *Etude Géologique de L’EPIRE (Grèce Nord-Occidentale)*; Technip eds.; Paris, France, 1966; p. 306.
67. Avramidis, P.; Zelilidis, A. The nature of deep-marine sedimentation and palaeocurrent trends as an evidence of Pindos foreland basin fill conditions. *Episodes* **2001**, *24*, 252–256.
68. Avramidis, P.; Zelilidis, A.; Vakalas, I.P.; Kontopoulos, N. Interactions between tectonic activity and eustatic sea-level changes in the Pindos and Mesohellenic Basins, NW Greece: Basin evolution and hydrocarbon potential. *J. Pet. Geol.* **2002**, *25*, 53–82.
69. Pantopoulos, G.; Vakalas, I.; Maravelis, A.; Zelilidis, A. Statistical analysis of turbidite bed thickness patterns from the Alpine fold and thrust belt of western and southeastern Greece. *Sed. Geol.* **2013**, *294*, 37–57, doi:10.1016/j.sedgeo.2013.05.007.

70. Karakitsios, V.; Roveri, M.; Lugli, S.; Manzi, V.; Gennari, R.; Antonarakou, A.; Triantaphyllou, M.; Agiadi, K.; Kontakiotis, G. Remarks on the Messinian evaporites of Zakynthos Island (Ionian Sea, Eastern Mediterranean). *Bull. Geol. Soc. Gr.* **2013**, *47*, 146–156.
71. Karakitsios, V.; Roveri, M.; Lugli, S.; Vinicio, M.; Rocco, G.; Antonarakou, A.; Triantaphyllou, M.; Agiadi, K.; Kontakiotis, G.; Kafousia, N.; et al. A record of the Messinian Salinity Crisis in the eastern Ionian tectonically-active domain (Greece, eastern Mediterranean). *Bas. Res.* **2017**, *29*, 203–233, doi:10.1111/bre.12173.
72. Karakitsios, V.; Tsaila-Monopolis, S. Données nouvelles sur les niveaux supérieurs (Lias inférieur-moyen) des Calcaires de Pantokrator (zone ionienne moyenne, Epire, Grèce continentale). Description des Calcaires de Louros. *Rev. Micropaleont.* **1988**, *31*, 49–55.
73. Danelian, T.; De Wever, P.; Azéma, J. Palaeoceanographic significance of new and revised palaeontological datings for the onset of Vigla Limestone sedimentation in the Ionian zone of Greece. *Geol. Mag.* **1997**, *134*, 869–872.
74. Karakitsios, V.; Tsikos, H.; van Breugel, Y.; Bakopoulos, I.; Koletti, L. Cretaceous oceanic anoxic events in western continental Greece. *Bull. Geol. Soc. Gr.* **2004**, *34*, 846–855.
75. Skourtsis-Coroneou, V.; Solacios, N.; Constantinidis, I. Cretaceous stratigraphy of the Ionian Zone, Hellenides, western Greece. *Cretac. Res.* **1995**, *16*, 539–558.
76. BP (British Petroleum) Co., Ltd. The geological results of petroleum exploration in western Greece: Institute for Geology and Subsurface Research (now Institute of Geology and Mineral Exploration) *Spec. Rep.* **1971**, *10*, 1–73.
77. Dunham, R.J. Classification of Carbonate Rocks According to Depositional Texture. In *Classification of Carbonate Rocks*, W.E. Hamm ed.; A Symposium, American Association of Petroleum Geologists: 1962; Tulsa Memoir 1, Tulsa, pp. 108–121.
78. Embry, A.F.; Klovan, J.E. A late devonian reef tract on northeastern banks island. *N.W.T. Bull. Can. Pet. Geol.* **1971**, *19*, 730–781, doi:10.11575/PRISM/22817.
79. Wilson, J.L. *Carbonate Facies in Geological History*; Springer: Berlin/Heidelberg, Germany, 1975; p. 471.
80. Buxton, M.W.N.; Pedley, H.M. A standardized model for Tethyan Tertiary carbonates ramps. *J. Geol. Soc.* **1989**, *146*, 746–748, doi:10.1144/gsjgs.146.5.0746.
81. Burchette, T.P.; Wright, V.P. Carbonate ramp depositional systems. *Sediment. Geol.* **1992**, *79*, 3–57, doi:10.1016/0037-073890003-A.
82. Pedley, M. A review of sediment distributions and processes in Oligo-Miocene ramps of southern Italy and Malta (Mediterranean divide). *Geol. Soc. London Spec. Publ.* **1998**, *149*, 163–179, doi:10.1144/GSL.SP.1999.149.01.09.
83. Pomar, L. Types of carbonate platforms: A genetic approach. *Basin Res.* **2001**, *13*, 313–334, doi:10.1046/j.0950-091x.2001.00152.x.
84. Flügel, E. *Microfacies Analysis of Limestones: Analysis, Interpretation and Application*; Springer Verlag: Berlin, Germany, 2004; p. 976.
85. Flügel, E. *Microfacies Analysis of Carbonate Rocks*; Springer Verlag: Berlin, Germany, 2010, p. 745.
86. Moforis, L. Stratigraphy, Reservoir Characteristics and Paleogeographic Distribution of the Triassic to Eocene Carbonates in Western Greece and Albania, Based on Field, Laboratory and Well Data. Master's Thesis, National and Kapodistrian University of Athens, 2016, Athens, Greece, pp. 1–122.
87. I.G.S.R. *Geological Map of Greece Series, Pappadaitai Sheet, Scale 1:50.000*; Institute for Geology and Subsurface Research: Athens, Greece, 1966.
88. I.G.S.R. *Geological Map of Greece Series, Ioannina Sheet, Scale 1:50.000*; Institute for Geology and Subsurface Research: Athens, Greece, 1967.
89. I.G.S.R. *Geological Map of Greece Series, Doliana Sheet, Scale 1:50.000*; Institute for Geology and Subsurface Research: Athens, Greece, 1968.
90. I.G.S.R. *Geological Map of Greece Series, Tsepelovo Sheet, Scale 1:50.000*; Institute for Geology and Subsurface Research: Athens, Greece, 1970.
91. Ahr, W.M. *Geology of Carbonate Reservoirs: The identification, description, and characterization of Hydrocarbon Reservoirs in Carbonate Rocks*; A John Wiley & Sons, INC., Publication, Texas A&M University: Hoboken, New Jersey, 2008.

92. Brown, A. Porosity variation in carbonates as a function of depth: Mississippian Madison Group, Williston basin. In *Reservoir Quality Prediction in Sandstones and Carbonates*; Kupecz, J.A., Gluyas, J., Bloch, S., Eds.; AAPG Memoir: Tulsa, Oklahoma, 1997; Volume 69, pp. 29–46.
93. Ehrenberg, S.N.; Nadeau, P.H. Sandstone versus carbonate petroleum reservoirs: A global perspective on porosity-depth and porosity-permeability relationships. *AAPG Bull.* **2005**, *89*, 435–445.
94. Ehrenberg, S.N.; Eberli, G.P.; Keramati, M.; Moallemi, S.A. Porosity-permeability relationships in interlayered limestone-dolostone reservoirs. *Am. Assoc. Pet. Geol. Bull.* **2006**, *90*, 91–114, doi:10.1306/08100505087.
95. Budd, D.A. Permeability loss with depth in the Cenozoic carbonate platform of west-central Florida. *AAPG Bull.* **2001**, *85*, 1253–1272.
96. Hosa, A.; Wood, R.A.; Corbett, P.W.M.; Souza, R.S.; Roemers, E. Modelling the impact of depositional and diagenetic processes on reservoir properties of the crystal-shrub limestones in the 'Pre-Salt' Barra Velha Formation, Santos Basin, Brazil. *Mar. Petr. Geol.* **2020**, *112*, 104100, doi:10.1016/j.marpetgeo.2019.104100.
97. Gudmundsson, A. *Rock Fractures in Geological Processes*; Cambridge University Press: United Kingdom, 2011.
98. Jaeger, J.C.; Cook, N.G.W.; Zimmerman, R.W. *Fundamentals of Rock Mechanics*; Blackwell Publishing: Oxford, United Kingdom, 2007.
99. Mavko, G.; Mukerji, T.; Dvorkin, J. *The Rock Physics Handbook: Tools for Seismic Analysis of Porous Media*; Cambridge University Press: United Kingdom, 2009.
100. Karakitsios, V.; Rigakis, N.; Bakopoulos, I. Migration and trapping of the Ionian series hydrocarbons (Epirus, NWGreece). *Bull. Geol. Soc. Gr.* **2001**, *34*, 1237–1245.
101. Bourli, N.; Kokkaliari, M.; Iliopoulos, I.; Pe-Piper, G.; Piper, D.J.W.; Maravelis, A.G.; Zelilidis, A. Mineralogy of siliceous concretions, cretaceous of Ionian zone, western Greece: Implication for diagenesis and porosity. *Mar. Pet. Geol.* **2019**, *105*, 45–63, doi:10.1016/j.marpetgeo.2019.04.011.
102. Karakitsios, V.; Koletti, L. Critical Revision of the Age of the Basal Vigla Limestones (Ionian Zone, Western Greece), Based on Nannoplankton and Calpionellids, with Paleogeographical Consequences. In *Knihovnicka Zemniho Plynu a Nafty, Proceedings of the 4th International Nannoplankton Association Conference, Prague, Czech Republic, September 1992*; Hamrsmid, B., Young, J. Eds.; Knihovnicka ZPN, 14a, Volume 14a, pp. 165–177.
103. BouDagher-Fadel, M.K. Evolution and Geological Significance of Larger Benthic Foraminifera. *Dev. Palaeontol. Stratigr.* **2008**, *21*, 1–548.
104. Höntzsch, S.; Scheibner, C.; Kuss, J.; Marzouk, A.M.; Michael, W.; Rasser, M.W. Tectonically driven carbonate ramp evolution at the southern Tethyan shelf: The Lower Eocene succession of the Galala Mountains, Egypt. *Facies* **2011**, *57*, 51–72.
105. Haq, B.U.; Hardenbol, J.; Vail, P.R. Chronology of fluctuating sea levels since the Triassic. *Science* **1987**, *235*, 1156–1166.
106. Miller, K.G.; Mountain, G.S.; Wright, J.D.; Browning, J.V. A 180-million-year record of sea level and ice volume variations from continental margin and deep-sea isotopic records. *Oceanography* **2011**, *24*, 40–53, doi:10.5670/oceanog.2011.26.
107. Kontakiotis, G.; Karakitsios, V.; Cornée, J.; Moissette, P.; Zarkogiannis, S.D.; Pasadakis, N.; Koskeridou, E.; Manoutsoglou, E.; Drinia, H.; Antonarakou, A. Preliminary results based on geochemical sedimentary constraints on the hydrocarbon potential and depositional environment of a Messinian sub-salt mixed siliciclastic-carbonate succession onshore Crete (Plouti section, eastern Mediterranean). *Med. Geosc. Rev.* **2020**, *2*, 247–265, doi:10.1007/s42990-020-00033-6.
108. Grohmann, S.; Fietz, W.; Nader, F.; Romero-Sarmiento, M.; Baudin, F.; Littke, R. Characterization of Late Cretaceous to Miocene source rocks in the Eastern Mediterranean Sea: An integrated numerical approach of stratigraphic forward modeling and petroleum system modeling. *Basin Res.* **2020**, doi:10.1111/bre.12497.

